Sub-chronic effects of AgNPs and AuNPs on Gammarus fossarum (Crustacea Amphipoda): From molecular to behavioural responses

Kahina Mehennaoui, Sébastien Cambier, Laetitia Minguez, Tommaso Serchi, Francois Guerold, Arno C Gutleb, Laure Giamberini

Ecotoxicology and Environmental Safety 210 (2021) 111775

Contents lists available at ScienceDirect

Ecotoxicology and Environmental Safety

journal homepage: www.elsevier.com/locate/ecoenv

Sub-chronic effects of AgNPs and AuNPs on *Gammarus fossarum* (Crustacea Amphipoda): From molecular to behavioural responses

Kahina Mehennaoui [a,b], Sébastien Cambier [a], Laëtitia Minguez [b], Tommaso Serchi [a], François Guérold [b], Arno C. Gutleb [a], Laure Giamberini [b,*]

[a] Environmental Research and Innovation (ERIN) Department, Luxembourg Institute of Science and Technology, 41 rue du Brill, Belvaux, Luxembourg
[b] Université de Lorraine, CNRS UMR 7360, Laboratoire Interdisciplinaire des Environnements Continentaux (LIEC), Campus Bridoux, Rue du Général Delestraint, F-57000, Metz, France

ARTICLE INFO

Edited by Professor Bing Yan

Keywords:
Gammarus fossarum, silver nanoparticles
Gold nanoparticles
Gene expression
Digestive lysosomal system
Osmoregulation
Behaviour
Cytoviva®
Long term exposure

ABSTRACT

The aim of the present study was the assessment of the sub-chronic effects of silver (AgNPs) and gold nanoparticles (AuNPs) of 40 nm primary size either stabilised with citrate (CIT) or coated with polyethylene glycol (PEG) on the freshwater invertebrate *Gammarus fossarum*. Silver nitrate ($AgNO_3$) was used as a positive control in order to study the contribution of silver ions potentially released from AgNPs on the observed effects. A multibiomarker approach was used to assess the long-term effects of AgNPs and AuNPs 40 nm on molecular, cellular, physiological and behavioural responses of *G. fossarum*. Specimen of *G. fossarum* were exposed for 15 days to 0.5 and 5 μg L^{-1} of CIT and PEG AgNPs and AuNPs 40 nm in the presence of food. A significant uptake of both Ag and Au was observed in exposed animals but was under the toxic threshold leading to mortality of *G. fossarum*. Silver nanoparticles (CIT-AgNPs and PEG-AgNPs 40 nm) led to an up-regulation of *Na^+K^+ATPase* gene expression. An up-regulation of *Catalse* and *Chitinase* gene expressions due to exposure to PEG-AgNPs 40 nm was also observed. Gold nanoparticles (CIT and PEG-AuNPs 40 nm) led to an increase of *CuZnSOD* gene expression. Furthermore, both AgNPs and AuNPs led to a more developed digestive lysosomal system indicating a general stress response in *G. fossarum*. Both AgNPs and AuNPs 40 nm significantly affected locomotor activity of *G. fossarum* while no effects were observed on haemolymphatic ions and ventilation.

1. Introduction

The recent advances in nanotechnologies led to an increasing use of engineered nanoparticles (ENPs) in various consumer products. Silver nanoparticles (AgNPs) are among the most promising and most widely used ENPs due to their broad spectrum antimicrobial activities (Vance et al., 2015). They are currently found in many products of daily life such as textiles, plastics, health care products, water filters or food packaging. Gold nanoparticles (AuNPs) are used in a wide range of applications in the field of biomedicine, biology and chemistry (Nel et al., 2006; Smita et al., 2012; Volland et al., 2015) mostly because of their potential low toxicity and probable high bio-compatibility (García-Cambero et al., 2013; Lapresta-Fernández et al., 2012). The increased production and use of AgNPs and AuNPs has raised concerns about their release in the environment (Farkas et al., 2011; Kaegi et al., 2010). The predicted environmental concentrations in surface water for both AgNPs and AuNPs are expected to be in the range from 0.01 μg L^{-1} to 0.32 μg L^{-1} and from 0.14 μg L^{-1} to 1.43 μg L^{-1}, respectively (Gottschalk et al., 2013; Tiede et al., 2009; Yang et al., 2016). Nanoparticles present unique physical-chemical properties in terms of size, shape, surface coatings and charges that will substantially influence their behaviour, fate and their effects/toxicity towards living organisms (Bai and Tang, 2020; McGillicuddy et al., 2017). Their potential uptake and entry into cells may lead to general stress as well as the generation of reactive oxygen species (ROS) resulting in oxidative stress that has been reported as one of the principal mechanisms of toxicity of NPs in aquatic organisms (Klaine et al., 2008; Vale et al., 2016; Volland et al., 2015).

Many studies have investigated the impacts of AgNPs and AuNPs on key freshwater species (Artal et al., 2020). Most of the studies focused on acute toxicity through direct exposure (Buffet et al., 2013). However, in order to better predict the potential effects of ENPs at higher biological levels, such as population and community levels, it is important to

* Correspondence to: Laboratoire Interdisciplinaire des Environnements Continentaux, Université de Lorraine, 8 rue du General Delestraint, Campus Bridoux, 57000 Metz, France.
E-mail address: laure.giamberini@univ-lorraine.fr (L. Giamberini).

https://doi.org/10.1016/j.ecoenv.2020.111775
Received 4 August 2020; Received in revised form 4 December 2020; Accepted 5 December 2020
Available online 8 January 2021

include food and assess the chronic toxicity of these ENPs through a multi-biomarker approach (Blinova et al., 2012; Gaiser et al., 2011; Mackevica et al., 2015). It is recognised that one important uptake route for metals and particles is through nutrition (Croteau et al., 2011; Luoma et al., 2014; Luoma and Rainbow, 2005). Silver was found in the form of NPs in the gut of polychaete exposed through the diet to AgNPs (García-Alonso et al., 2014). Some studies reported effects of AgNPs and AuNPs after trophic exposure of aquatic organisms. Trophic exposure of the clam *Corbicula fluminae* to AuNPs led to NPs presence in the epithelia of the digestive gland and gills of the animals (Renault et al., 2008). Additionally, an activation of phase II antioxidant enzymes encoding genes and an increase in metallothionein gene expression was observed (Renault et al., 2008). Trophic exposure (15 days) of zebrafish to sub-lethal concentrations of AgNPs 20 nm resulted in a significant Ag accumulation in liver blood vessels and in the interstitial tissue between the intestine and the liver. Gene expression profiles revealed that AgNPs 20 nm impacted photo-transduction system, circadian clock regulation and photoreception (Cambier et al., 2018).

Amphipods of the genus *Gammarus* such as *Gammarus fossarum* represent an important part of the aquatic macroinvertebrate assemblage (Dedourge-Geffard et al., 2009; Ladewig et al., 2006). *Gammarus fossarum* have been used as a model species due to their wide distribution in Europe (Janetzky, 1994) and their major functional role in litter breakdown process and nutrient cycling (Forrow and Maltby, 2000; Kelly et al., 2002; Lacaze et al., 2010; MacNeil et al., 1997). The ease of use, identification to the species level, differentiation between gender, sampling and laboratory handling in addition to the well-documented sensitivity to different kind of pollutants make *Gammarus* a good model organism for ecotoxicological studies (Arce Funck et al., 2013; Mehennaoui et al., 2016, 2018a; Lüderwald et al., 2019). In our previous study, influence of size and surface coatings on the acute toxicity of AgNPs and AuNPs were assessed (Mehennaoui et al., 2018a). Acute exposure of *G. fossarum* to AgNPs and AuNPs showed: (i) a coating dependent bio-accumulation, which was higher for citrate stabilised NPs as compared to polyethylene glycol-coated (PEG) NPs; (ii) a metal dependent tissues distribution, with AgNPs found in *G. fossarum* gills while AuNPs were found in intestinal caeca; and (iii) an induction of antioxidant genes by AgNPs, while AuNPs led to their down regulation. However, the previous study only investigated the acute effects of AgNPs and AuNPs, but there is still a lack of information about the chronic toxicity of AgNPs and AuNPs in *G. fossarum*. Hence, the aim of the present study was to investigate the chronic toxicity of differently coated AgNPs and AuNPs 40 nm (citrate (CIT) and polyethylene glycol (PEG) as surface coatings) on *G. fossarum*. Effects of $AgNO_3$ were also studied in order to determine the contribution of the released silver ions to the observed biological effects. A multibiomarker approach including molecular effects (stress-related gene expression), cellular (response of the digestive lysosomal system (DLS)), physiological (osmoregulation) and behavioural (locomotion and ventilation) responses was used (Mehennaoui et al., 2016). Mortality and Ag and Au bioaccumulation were also assessed. The integrative approach applied in the current study aims also to identify a potential adverse outcome pathway (AOP) for AgNPs and AuNPs toxicity on *G. fossarum*.

2. Organisms, materials and methods

2.1. Particles and chemicals

Citrate stabilised AgNPs (CIT-AgNPs 40 nm) and citrate stabilised AuNPs (CIT-AuNPs 40 nm) were purchased from Nanocomposix (San Diego, USA). Coating of AgNPs and AuNPs with PEG was performed at the Material Research and Technology (MRT) Department of the Luxembourg Institute of Science and Technology (LIST) following a wet chemistry method as described in our previous study (Mehennaoui et al., 2018a). Silver nitrate ($AgNO_3$) (CAS no.7761-88-8) was purchased from Merck-VWR (Leuven, Belgium). The embedding resin Cryomatrix® (Cat no 6769006) was purchased from ThermoFisher Scientific (illkirch, France).

2.2. Particle characterisation

Size distribution of CIT-AgNPs, PEG-AgNPs, CIT-AuNPs and PEG-AuNPs 40 nm in mineral water (exposure medium in presence of food, Volvic®), at T0h and T72h, were characterised using Nanoparticle Tracking Analysis (NTA), measured on a NanoSIGHT instrument (Malvern Instrument Ltd, UK) using harmonised protocols (Hole et al., 2013; Maguire et al., 2017). Size distribution of CIT-AgNPs, PEG-AgNPs, CIT-AuNPs and PEG-AuNPs 40 nm in Volvic water in absence of food was also characterised and presented in our previous study (Mehennaoui et al., 2018a).

2.3. Alder leave conditioning

Leaves of alder (*Alnus glutinosa*) were collected at abscission from the riparian vegetation of La Maix stream (436 m a.s.l; 48.483874° N, Long: 7.038951° E), which is a reference stream located in the Vosges Mountains (North-Eastern France), air-dried and kept at room temperature until use. Leaves were rinsed in deionized water for 5 min and cut into 16 mm diameter discs. Sets of 50 leaf discs were placed into fine-net bags (0.5 mm pore size) and immersed in an unpolluted stream (Schwaarzbaach, Colmar-berg, Luxembourg, 49°48′24.9′’ N and 06°04′53.2′’ E,) (Dohet et al., 2008; Mehennaoui et al., 2016, 2018a, 2018b) for 10 days to allow microbial colonisation. At the end of the immersion period, leaves were returned to the laboratory and were kept at − 20 °C until use (Andreï et al., 2016; Batista et al., 2017).

2.4. Organism sampling and acclimation

Gammarus fossarum were collected in November 2016 at the same unpolluted site in Schwaarzbaach as in our previous studies (Mehennaoui et al., 2018a, 2016). Adult animals were collected using a hand net and were sorted in the field to separate males, which were used for the experiments, from females, which were immediately returned to the water stream. Collected male animals were transported to the laboratory in plastic tanks filled with river water. Once in the laboratory, they were kept overnight at 12 °C before acclimation (Mehennaoui et al., 2018a, 2016).

The rationale for choosing adult males is that this selection allows avoiding influence of gender and reproduction cycle on the studied parameters (Arce Funck et al., 2013; Sornom et al., 2010). *Gammarus fossarum* males were selected from pre-copula pairs or based on sexual dimorphism like gnatopode size (Mehennaoui et al., 2016). Adult males (average size = 10.8 ± 0.5 mm) were then acclimated to laboratory conditions (Andreï et al., 2016; Mehennaoui et al., 2016). The acclimation was conducted in 2 steps. First, Gammarids were acclimated for 72 h to mineral water (Volvic, France) by progressively changing field water to Volvic water (30% vol/vol, 50% vol/vol, 100% vol/vol), every 24 h. Then, a stalling period of 10 days was conducted in 100% Volvic water (Andreï et al., 2016; Mehennaoui et al., 2016). Acclimation was performed under controlled conditions at 12 °C with a 16 h light 8 h dark photoperiod. 100% of Volvic water was aerated and completely changed every 24 h to avoid organic matter accumulation and potential increase of ammonium, nitrite and nitrate. Gammarids were fed ad libitum with alder leaves collected from the same unpolluted site.

2.5. Sub-chronic toxicity test

2.5.1. Experimental design

In order to avoid as much as possible the adsorption of the chemicals used for the exposure on the tank walls (either $AgNO_3$, AgNPs 40 nm and AuNPs 40 nm), the tanks used for exposure were pre-saturated with $AgNO_3$, AgNPs 40 nm and AuNPs 40 nm for 96 h before exposure.

At the end of the acclimation period, groups consisting of 15 males were transferred into the pre-saturated plastic tanks (500 mL polypropylene tanks) containing 400 mL of exposure medium (Volvic water with or without contaminants) (Mehennaoui et al., 2016) and 6 alder leave discs as food. A piece of mesh (0.5 mm pore size) was added in each tank to provide a resting surface for *G. fossarum* and to reduce as much as possible potential deaths linked to cannibalism. Males were exposed to different treatments: $AgNO_3$ (0–0.5 μg L^{-1}); CIT-AgNPs 40 nm, PEG-AgNPs 40 nm, CIT-AuNPs 40 nm and PEG-AuNPs 40 nm (0–0.5 −5 μg L^{-1}) for 15 days at 12 °C with a photoperiod of 16 h light and 8 h darkness. The different ranges of concentrations tested were selected based on previous results obtained by exposing *G. fossarum* to the same Ag and Au nanoparticles for 72 h (Mehennaoui et al., 2018a) and on the predicted environmental concentrations. Stock solutions of $AgNO_3$, AgNPs and AuNPs were diluted to the desired concentrations in mineral water (Volvic, France). 100% of exposure medium were renewed every 72 h to maintain the exposure conditions stable, to ensure sufficient amount of nutrients and to remove waste products. Dead animals were removed, and survivors were counted every 24 h. Six leave discs per replicate were added every 48 h to replace the eaten ones (Fig. S1).

2.5.2. Silver and gold concentrations in G. fossarum's tissue

At the end of the exposure period, three pools of gammarids, 4 for each condition, were rinsed with Milli-Q water and gently dried on filter paper. Animals were frozen at − 20 °C, freeze-dried and weighed. Samples were then mineralised in HNO_3 and H_2O_2 for Ag measurement and in acidic mixture of HNO_3 and HCl (aqua Regia) for Au measurement at a maximum pressure of 35 bars and maximum temperature of 200 °C using a microwave system (Anton Paar Multiwave Pro) as previously described (Mehennaoui et al., 2016, 2018b). All measurements were performed in triplicate and are expressed in μg g^{-1} of dry weight. A calibration curve was performed following serial dilutions (from 0.01 to 50 μg L^{-1} of Ag and from 0.025 to 10 μg $L^{-1}$for Au). Using a multi-element standard solution (Chemlab, certified ISO/IEC 17025). The validity of the analytical method was controlled every 10 measurements within the same series of measurements with 3 quality controls (0.5, 5 and 25 μg L^{-1} of Ag and Au) of a second multi-element standard solution (Merck-VWR, ISO/IEC 17025). Values of Ag and Au were consistent within the certified ranges (Cambier et al., 2018).

2.5.3. Molecular effects

2.5.3.1. RNA extraction and cDNA synthesis. At the end of the exposure period, animals were gently dried and flash-frozen in liquid nitrogen in RNA lysis Buffer (RLT buffer) supplemented with 1% (vol/vol) β-mercaptoethanol, and stored at − 80 °C until RNA extraction. Tissues of *G. fossarum* were grinded on ice using a pellet pestle tissue grinder and the homogenates were centrifuged at 250*g* for 5 min at 4 °C to remove cuticle fragments as previously described (Mehennaoui et al., 2016). Total RNA was extracted using RNeasy mini kit for cells and animal tissues (Qiagen, Leusden, The Netherlands), according to the manufacturer's instructions (including digestion with DNase). Concentrations and purity of RNA were assessed measuring the absorbance at 230, 260 and 280 nm using a Nanodrop ND-1000 spectrophotometer (Thermo Fisher Scientific, Waltham, MA, USA) (A260/280 and A260/230 ratios). Integrity of RNA was controlled using the RNA Nano 6000 assay (Agilent Technologies, Diegem, Belgium) on a 2100 Bioanalyzer instrument (Agilent, Santa Clara, CA, USA) (Legay et al., 2015). For the synthesis of cDNA, 1 μg of the extracted RNA were retro-transcribed into cDNA using the Protoscript II reverse transcriptase (New England Biolabs, Leiden, The Netherlands) and random primers, according to the manufacturer's instructions.

2.5.3.2. Primer design and quantitative real-time PCR. All primers for the RT-qPCR were designed using the software Primer3Plus (http://primer3.ut.ee) with the previously described criteria (Mehennaoui et al., 2018a, 2018b). Primers were analysed using NetPrimer (http://www.premierbiosoft.com/netprimer/) for secondary unexpected structures. Verification of PCR efficiency was performed using decreasing five-fold dilutions from cDNA pool (From 25 ng to 0.04 ng and no template control). Melting curves were generated at the end of each experiment to assess the specificity of the amplified products. All primers displayed one clear peak and were all retained for the analysis. All the used primers are described in our previous study (Mehennaoui et al., 2018a, 2018b).

The cDNAs were diluted to 0.8 ng μL^{-1} and used for RT-qPCR analyses in 384-well plates. An automated liquid handling robot (epMotion 5073, Eppendorf, Hamburg, Germany) was used for the preparation of the 384-well plate. The cDNAs were amplified using Takyon Low ROX SYBR MasterMix dTTP Blue Kit (Eurogentec, Liège, Belgium) on a ViiA 7 Real-Time PCR System (Thermo Fisher Scientific, Waltham, MA, USA) in a final volume of 10 μL (Behr et al., 2015). All reactions were performed in three technical replicates each one including four biological replicates. The PCR conditions consisted on an initial denaturation step at 95 °C for 3 min, followed by 40 cycles of denaturation at 95 °C for 15 s and annealing/extension steps at 60 °C for 1 min. Two genes, namely *Clathrin and SDH*, were selected among six genes to be used as reference and they were validated using the GeNorm module in the Biogazelle qBase PLUS software (Mehennaoui et al., 2018b). The relative gene expression was calculated including PCR efficiency using Biogazelle qbase Plus software 2.5 with the $^{\Delta\Delta}$CT method.

2.5.4. Morphology of the digestive lysosomal system

2.5.4.1. Sample preparation. At the end of exposure period, four pools for 4 gammarids per condition were used for assessing the response of the digestive lysosomal system. Intestinal caeca were manually dissected from each *Gammarus*. Tissues were cryoprotected in phosphate buffer solution (0.05 M, pH 7.4) containing 7% sucrose (vol/vol). Samples were embedded in Cryomatrix® embedding resin and stored at − 80 °C until analysis (Giambérini and Cajaraville, 2005a).

2.5.4.2. Histochemistry and stereology. The removed gut caeca were used to quantify the structural changes of the digestive lysosomal system (DLS), as measure of the activity of the β-glucuronidase enzyme in unfixed cryostat tissue sections (Cajaraville et al., 1991; Giambérini and Cajaraville, 2005a). Measurements were performed on digestive tissue sections of 8 μm thickness by image analysis using the software Cell* Olympus) using a Sony DP50 colour video camera connected to an Olympus BX41 microscope with a 100x magnification. Eight fields of view were randomly selected and examined on two sections per individual in each experimental group for a total sampling area per organism of 98.715 μm^2. Areas not belonging to caeca were removed from analyses. Four stereological parameters of lysosome were calculated: the volume density ($V_v = V_L/V_C$), the surface density ($S_v = S_L/V_C$), the surface to volume ratio ($S/V = S_L/V_L$, corresponding to the inverse of lysosome size) and the numerical density ($N_v = N_L/V_C$). C corresponds to digestive cell cytoplasm, L corresponds to lysosomes, N to numbers, S to surface and V to volume (Minguez et al., 2009).

2.5.5. Particle uptake: Cytoviva ® dark field hyperspectral imagining analyses

Cryo-sections used for the quantification of the DLS were used to assess particle uptake in *G. fossarum* exposed to AgNPs and AuNPs. Measurements were performed on digestive tissue sections of 8 μm thickness on Cytoviva dark field hyperspectral imaging system (Cytoviva Inc., Auburn, Alabama, USA).

Slides were covered with a glass cover slip and kept at room temperature until analyses. Digestive tissues were visualised using a Cytoviva® darkfield hyperspectral imaging system mounted on an Olympus

BX-43 optical microscope. Images of the digestive tissues of *G. fossarum* were captured at 60x magnification with oil immersion using hyperspectral camera controlled by ENVI software (version 4.8 from Harris Corporation, Melbourne, FL, USA and modified by CytoViva, Inc.). Spectral libraries of exposed animals were generated manually acquiring about 200 spectra per sample. Acquired libraries were filtered against non-exposed samples to filter out all spectra non-related to AgNPs or AuNPs using a spectral angle mapper (SAM) algorithm with a 0.1 radians tolerance. Filtered libraries were mapped onto images of exposed samples using SAM with a 0.1 radians tolerance which allows highlighting similarities between the spectra in the image and in the spectral library (Mehennaoui et al., 2018a).

2.5.6. Behavioural responses and osmoregulation

For each treatment, measurements of locomotor activity, ventilation and osmoregulation were performed on the same pool of 10 organisms (Mehennaoui et al., 2016).

2.5.6.1. Locomotor activity. At the end of the exposure period, locomotor activity was firstly assessed by counting the number of animals in movement in a 80 mL glass tank containing 10 organisms with a piece of net added to provide a resting surface (Felten et al., 2008). Measurements were performed after 5 min of acclimation at the same time of the day with similar light conditions and in a quiet environment. Moving *G. fossarum* were counted for a period of 2 s and this process was repeated 40 times (Mehennaoui et al., 2016).

2.5.6.2. Ventilation activity. Ventilation activity was recorded immediately after locomotion on the same animals, by measuring the frequency of pleopod beats. Ten gammarids from each treatment group were placed individually in a glass tube containing Volvic water and left for a 30 s acclimation period. Then, pleopod beats were visually counted three times for 10 s, using a manual cell counter, only when animals were at rest. Measurements were performed at the same period of the day to avoid possible effects of a circadian rhythm on respiration (Felten et al., 2008; Mehennaoui et al., 2016; Rosas et al., 1992).

2.5.6.3. Osmoregulation

2.5.6.3.1. Haemolymph sampling. Immediately after behavioural response measurements, animals were dried on filter paper. Samples of haemolymph were taken from the telson of each individual (n = 10) using a modified microcapillary (Felten et al., 2008). To prevent haemolymph coagulation, samples were kept at 4 °C until Na^+ and Cl^- measurements (Arce Funck et al., 2013).

2.5.6.3.2. Haemolymph Na^+ and Cl^- concentration measurements. Samples of haemolymph (0.8–1.2 μL) were transferred to a gauged 5 μL microcapillary tube and were centrifuged for 10 min at 6600*g* at 4 °C. Samples were then diluted in 2.5 mL of Milli-Q water to determine Na^+ concentrations using atomic absorption spectrophotometry (Perkin Elmer Analyst 100) and Cl^- concentrations using ionic chromatography (Dionec 4500i equipped with an Ion Pac AS4A column) (Arce Funck et al., 2013; Felten et al., 2008).

2.6. Statistical analyses

All results are reported as mean ± SD (standard deviation). Results of locomotor activity were obtained from the same set of individuals. Therefore, a one-way ANOVA with repeated measurements following a general linear model was used as statistical test. The observed Ag and Au bioaccumulation, survival, ventilation and gene expression on $\log_2$ transformed normalised relative quantities were compared using a one-way ANOVA followed by Tukey-HSD *post-hoc* test for multiple comparisons when normality and homogeneity of variances were respected. When this was not the case, a non-parametric Kruskal-Wallis ANOVA followed by a Mann-Whitney *U* test was used. Statistical calculations were performed using Statistica software 12 (StatSoft Inc.).

All lysosomal statistical analyses were performed on RStudio (1.0.153). A Wilcoxon test was first run between non-contaminated control groups. As no differences were highlighted, the data were pooled (control n = 6). Moreover, due to technical limitations leading to low sample sizes, we calculated bootstrapped 95% confidence intervals (CIs) of the difference between group medians (BCa method, R = 1000). When the 95%CIs of the difference in medians excluded zero, we concluded that there was a statistically significant difference in median values between groups.

3. Results

3.1. Particle characterisation

In our previous study, CIT-AgNPs, PEG-AgNPs 40 nm were the most stable in Volvic water with hydrodynamic diameter of 45 ± 1.5 and 47 ± 1.3 nm, respectively (Mehennaoui et al., 2018a). Hydrodynamic diameter of CIT-AuNPs 40 nm was of 67 ± 13 nm after 24 h in Volvic water, and PEG-AuNPs size after 24 h in Volvic water was 38 ± 19 nm (Mehennaoui et al., 2018a). In the present study, particle size characterisation at 5 μg L^{-1} of CIT-AgNPs, PEG-AgNPs, CIT-AuNPs and PEG-AuNPs 40 nm in Volvic water in presence of food was impossible as we were under the limits of detection of the NanoSIGHT. However, NPs characterisation at 100 μg L^{-1} of CIT-AgNPs 40 nm and CIT-AuNPs 40 nm in Volvic water in presence of food did not allow the distinction between NPs and food particles. As shown in supplementary material (Fig. S2A), after 24 h in Volvic water in presence of food, CIT-AgNPs 40 nm showed several peaks of different sizes, while after 72 h, a majority of particles with a hydrodynamic diameter of about 100 nm were detected although it was impossible to distinguish between metallic NPs and organic matter (Fig. S2B).

3.2. Survival

Survival rates following exposure time (15 days) were stable in all the exposure conditions (Table 1). Only 0.5 μg L^{-1} of $AgNO_3$ led to a significant decrease of 35 ± 3.3%, in survival rates of *G. fossarum* at day 15 (One-way ANOVA, F = 11.63, 8df, $P < 0.001$) (Table 1).

3.3. Silver and gold concentrations in G. fossarum tissue

At the end of the exposure period, Ag was detected in the negative control groups of *G. fossarum* (0.24 ± 0.1 μg g^{-1} d.w.) (Table 1).

Table 1
G. fossarum Ag and Au uptake and survival rate (mean ± SD) after 15 days of exposure to CIT and PEG-AgNPs and AuNPs 40 nm.

Compound		Nominal concentrations ($\mu g.L^{-1}$)	*Gammarus* internal [Ag] and [Au] ($\mu g.g^{-1}$ gammarids dw)	Survival rate (%, Mean ± SD)
AgNPs 40 nm	CIT	0	0.24 ± 0.01 ^{a}	80 ± 9.4^{a}
		0.5	0.42 ± 0.05 ^{ab}	86.7 ± 5.4^{a}
		5	**2.09 ± 0.19** ^{c}	81.7 ± 11.4^{a}
	PEG	0	0.24 ± 0.01 ^{a}	80.0 ± 9.4a
		0.5	0.37 ± 0.28 ^{ab}	76.6±11.5^{a}
		5	**1.55 ± 0.28** ^{bc}	85.0± 11.4^{a}
AuNPs 40 nm	CIT	0	< LOQ ^{a}	85.0±6.4^{a}
		0.5	0.11 ± 0.01 ^{a}	76.7±3.8^{a}
		5	1.03 ± 0.18 ^{abc}	76.7±3.8^{a}
	PEG	0	< LOQ ^{a}	85.0±6.4^{a}
		0.5	0.10 ± 0.03 ^{a}	78.3±6.4^{a}
		5	0.63 ± 0.16 ^{ab}	81.7±6.4^{a}
$AgNO_3$		0	0.21 ± 0.04 ^{a}	80.0±6.7^{a}
		0.5	**5.16 ± 1.21** ^{d}	**65.0±3.3**^{b}

Different letters (a–d) indicate significant differences (one-way ANOVA + Tukey HSD post hoc test at $P < 0.05$ level of significance, n = 15 for survival rate). Bold values indicate significant differences compared to control G. fossarum.

Exposure to $AgNO_3$ (0.5 μg L^{-1}) lead to the highest concentration of Ag (5.16 ± 1.20 μg g^{-1} d.w.) in *G. fossarum* body. Treatment with the AgNPs resulted in a significant concentration-dependent Ag body concentration for both CIT-AgNPs and PEG-AgNPs 40 nm (One-way ANOVA, F = 45.12, 17df, $P < 0.01$) (Table 1). The Au concentration was under the limit of quantification (< 0.075 μg g^{-1} dw) in the non-exposed animals. Although higher concentrations of Au were measured in *G. fossarum* exposed to 5 μg L^{-1} of CIT and PEG-AuNPs 40 nm, the observed concentrations were not statistically significant ($P > 0.05$, Table 1).

3.4. Molecular effects

Both concentrations (0.5 and 5 μg L^{-1}) of PEG-AgNPs 40 nm led to a significant up-regulation of *catalase* and *chitinase* with a 2-fold increase. A significant up-regulation of *Na^+K^+ATPase* (1.5-fold increase) was caused by exposure to CIT-AgNPs and PEG-AgNPs 40 nm. The highest concentrations of CIT and PEG-AuNPs 40 nm (5 μg L^{-1}) led to a significant 2-fold increase of *CuZnSOD* gene expression (Table 2).

3.5. Effects on the digestive lysosomal system

Exposure of *G. fossarum* to 5 μg L^{-1} of CIT-AgNPs 40 nm led to a more developed DLS with higher volume and surface associated to bigger size (lower S/V) when compared to negative control (Fig. 1A). Moreover, a concentration-dependent effect was observed with bigger lysosomes in *G. fossarum* exposed to 5 μg L^{-1} of CIT-AgNPs 40 nm when compared to *G. fossarum* exposed to 0.5 μg L^{-1} of CIT-AgNPs 40 nm. A coating-dependent effect was also observed as organisms exposed to 5 μg L^{-1} of CIT-AgNPs 40 nm have bigger lysosomes than those exposed to 5 μg L^{-1} of PEG-AgNPs 40 nm (Fig. 1A).

Gammarus fossarum exposed to 0.5 μg L^{-1} of CIT-AuNPs 40 nm and 5 μg L^{-1} of PEG-AuNPs 40 nm presented a more developed lysosomal system (higher Vv and Sv with bigger lysosomes) with a lower numerical density compared to control group (Fig. 1B). A concentration-dependent effect of CIT-AuNPs was observed as *G. fossarum* exposed to 5 μg L^{-1} of CIT-AuNPs 40 nm presented a more developed lysosomal system with bigger lysosomes (Fig. 1B). Furthermore, a coating-dependent effects was observed as CIT-AuNPs led to a higher numerical density of lysosome in gammarids when compared to PEG-AuNPs and at the highest concentration (5 μg L^{-1}) bigger lysosomes were observed in *G. fossarum* exposed to CIT-AgNPs 40 nm when compared to PEG-AuNPs (Fig. 1B).

3.6. Cytoviva® dark field hyperspectral imaging

Coloured section of intestinal caeca of *G. fossarum* exposed to 5 μg L^{-1} of AgNPs and AuNPs, used for the DLS analyses, were used for the localisation of AgNPs and AuNPs in *G. fossarum* tissues (Figs. 2 and 3). Yellow and blue colours indicate the intestinal caeca tissue (Figs. 2A and 3A). Red dots indicate lysosomes (Figs. 2D and 3B). Intestinal caeca tissue showed spectra of 690 nm and spectra of lysosome was 590 nm (Figs. 2C and 3C). As described in the previous Section 3.5 (effects of the DLS), CIT-AgNPs and PEG-AgNPs led to the activation of the DLS although it was not possible to see the differences between the coatings (CIT vs PEG). However, it is clear that PEG-AuNPs led to a more developed DLS in gammarids than CIT-AuNPs. However, the coloration of the biological samples did not allow the detection of internalised AgNPs and AuNPs.

3.7. Behavioural responses and osmoregulation

3.7.1. Locomotion and ventilation activity

Gammarus fossarum exposed to CIT-AgNPs, PEG-AgNPs 40 nm, CIT-AuNPs and PEG-AuNPs 40 nm and $AgNO_3$ showed a significant reduced locomotor activity when compared to non-exposed animals (Fig. 4A, GLM - one-way ANOVA, $P < 0.05$). Animals exposed to 0.5 μg L^{-1} of CIT-AgNPs 40 nm showed a significant reduced locomotion activity when compared to *G. fossarum* exposed to 5 μg L^{-1} CIT-AgNPs 40 nm and 0.5 μg L^{-1} of $AgNO_3$ (GLM- Tukey-HSD post-hoc test, $P < 0.05$). At the highest concentration (5 μg L^{-1}), PEG-AgNPs 40 nm led to a significant decrease in locomotor activity compared to CIT-AgNPs 40 nm (GLM- Tukey-HSD post-hoc test, $P < 0.05$). A significant decrease in the number of moving Gammarids was observed when animals were exposed to 0.5 μg L^{-1} of CIT-AuNPs 40 nm compared to those exposed to 5 μg L^{-1} of CIT-AuNPs 40 nm (GLM- Tukey-HSD post-hoc test, $P < 0.05$). No significant concentration- effects were observed in Gammarids exposed to PEG-AuNPs 40 nm (0.5 and 5 μg L^{-1}) (GLM-Tukey-HSD post-hoc test, $P > 0.05$).

Pleopod beat frequency of *G. fossarum* exposed to 5 μg L^{-1} of CIT-AgNPs 40 nm and CIT-AuNPs 40 nm was not significantly affected by AgNPs, AuNPs and $AgNO_3$ (Fig. 4B, Kruskal-Wallis ANOVA, $P < 0.05$).

3.7.2. Osmoregulation

The basal level of haemolymphatic Cl^- in control gammarids was constant with values of 70.4, 101.9 and 95.5 mmol L^{-1} in the three different control groups. The basal levels of haemolymphatic Na^+ were 108.8, 169.4 and 114.2 mmol L^{-1} in the non-exposed animals (Table S1 in supplementary material). No significant effects of AgNPs and AuNPs 40 nm were observed on the concentration of the different haemolymphatic ions indicating that osmoregulation of *G. fossarum* was not impacted by the applied treatment (Kruskal-Wallis ANOVA, $P > 0.05$).

4. Discussion

The chronic toxicity of AgNPs and AuNPs on *G. fossarum* has hardly been explored. In the present study we investigated the sub-chronic effects of differently coated (CIT and PEG) AgNPs and AuNPs 40 nm on *G. fossarum*. Individuals were exposed to realistic environmental concentrations (0.5 and 5 μg L^{-1}) of AgNPs and AuNPs 40 nm for 15 days and in presence of food (leave disk of *A. glutinosa*). Silver and gold nanoparticles of 40 nm were selected based on the results of our previous study as they were the most stable in exposure medium and the NPs with the highest uptake rate by *G. fossarum* (Mehennaoui et al., 2018a). The studied endpoints included mortality, bioaccumulation, tissue distribution, gene expression, response of the digestive lysosomal system, osmoregulation and behavioural responses (locomotion and ventilation) in order to identify potential toxicity pathways of AgNPs and AuNPs (Fig. 5).

4.1. Particle characterisation

Silver and gold nanoparticles of 40 nm were characterised in the exposure media (Volvic water) that contained food debris. For the characterisation of the size distribution in water, we used the nanoparticle tracking analysis (NTA), which did not allow a full characterisation of the studied NPs at the used concentrations (5 μg L^{-1}) as they were under the limits of detection (Andreï et al., 2016). Moreover, the presence of the food debris interferes with the detection of particles. Feeding in the present experiment can be considered as an influencing/confounding factor on the behaviour of AgNPs and AuNPs as observed in previous studies (Mackevica et al., 2015; Sørensen et al., 2016). Potentially, AgNPs and AuNPs interact with the different compounds present in the exposure medium and may be complexed or aggregated (Andreï et al., 2016; Levard et al., 2012; Petersen et al., 2014) but further analyses are needed in order to verify this hypothesis. This behaviour makes the commonly used techniques for characterisation (DLS, NTA and electron microscopy) unsuitable for environmental samples analysis due to their detection limits (Farré et al., 2008; Gallego-Urrea et al., 2011; Yang et al., 2016). A combination of various techniques seems to be the most adapted methodology for a full characterisation of ENPs in complex environmental samples. For instance, combining imaging technique like Transmission Electron microscopy

Table 2
Relative gene expression of *G. fossarum* exposed for 15 days to CIT- and PEG-AgNPs 40 nm and CIT and PEG-AuNPs 40 nm.

Compound		Concentrations (μg.L^{-1})	Cytoskeleteon		Exoskeleton		Antioxidant defense		General stress
			Actin	*TUB*	*UB*	*Chitinase*	*CAT*	*CuZnSOD*	*GPx7*
$AgNO_3$		**0**	1 ± 0.36	1 ± 0.26	1 ± 0.12	1 ± 0.28	1 ± 0.24	1 ± 0.64	1 ± 0.16
		0.5	1.44 ± 0.58	1.33 ± 0.56	1.16 ± 0.26	0.71 ± 0.34	0.73 ± 0.34	0.66 ± 0.32	0.83 ± 0.16
AgNPs 40 nm	**Control**	**0**	1 ± 0.3	1 ± 0.24	1 ± 0.96	1 ± 0.22	1 ± 0.2	1 ± 0.3	1 ± 0.08
	CIT	**0.5**	0.56 ± 0.22	0.79 ± 0.18	1.33 ± 0.18	1.15 ± 0.24	1.02 ± 0.28	1.13 ± 0.16	0.8 ± 0.16
		5	0.74 ± 0.38	0.89 ± 0.08	0.93 ± 0.7	1.48 ± 0.6	1.43 ± 0.46	0.88 ± 0.38	0.92 ± 0.22
	PEG	**0.5**	0.77 ± 0.14	0.97 ± 0.44	1.09 ± 0.5	**2.17 ± 1.9**	**1.98 ± 1.66**	1.2 ± 0.06	0.84 ± 0.14
		5	0.77 ± 0.44	0.92 ± 0.24	0.58 ± 0.66	**1.68 ± 1.14**	**1.7 ± 1.26**	0.9 ± 0.64	0.88 ± 0.16
AuNPs 40 nm	**Control**	**0**	1 ± 0.38	1 ± 0.3	1 ± 0.44	1 ± 0.22	1 ± 0.12	1 ± 0.48	1 ± 0.22
	CIT	**0.5**	1.02 ± 0.32	0.93 ± 0.44	0.96 ± 0.12	1.2 ± 0.4	1.31 ± 0.48	**1.71 ± 0.7**	1.04 ± 0.32
		5	1 ± 0.42	0.77 ± 0.26	0.85 ± 0.12	1.46 ± 0.26	1.43 ± 0.18	1.21 ± 0.56	1.05 ± 0.24
	PEG	**0.5**	0.97 ± 0.08	0.61 ± 0.48	1.23 ± 0.1	1.29 ± 0.46	1.24 ± 0.54	1.25 ± 0.36	0.99 ± 0.16
		5	1.26 ± 0.4	0.94 ± 0.2	1 ± 0.28	1.42 ± 0.54	1.44 ± 0.46	**2.14 ± 1.08**	1.01 ± 0.16

Indicates significant ($P < 0.05$, one-way ANOVA followed by Tukey-HSD post-hoc test) up-regulation genes (fold change > 1.5).

(TEM) with single particle-ICP-MS (sp-ICP-MS) might be the most suitable combination to characterise ENPs in term of morphology, number, mass and dissolved concentration in complex environments (Abbas et al., 2020; Clark et al., 2019; Galhano et al., 2020).

4.2. Biological endpoints

Exposure of *G. fossarum* for 15 days to CIT and PEG-AgNPs and CIT- and PEG-AuNPs 40 nm in the presence of food led to a concentration-dependent uptake of Ag and Au. These findings are in agreement with those described in our previous study in which *G. fossarum* were exposed for 72 h to an increasing gradient of AgNPs and AuNPs presenting different sizes and coatings (Mehennaoui et al., 2018a). Dose-dependent accumulation was also reported in *G. roeseli* exposed for 72 h to 0.5 and 5 μg L^{-1} of CIT-AgNPs 10 and 60 nm (Andreï et al., 2016). *Gammarus fossarum* exposed to the highest concentration of CIT-AuNPs 40 nm (5 μg L^{-1}) tended to accumulate more Au than non-exposed animals and those exposed to PEG-AgNPs and PEG-AuNPs. The uptake of Ag and Au after a chronic exposure in *G. fossarum* suggest a potential transfer of these NPs in the food chain.

However, despite an uptake of Ag and Au, no significant effects on survival were observed when animals were exposed to CIT and PEG-AgNPs 40 nm and CIT and PEG-AuNPs 40 nm. The internal concentration of Ag recorded in *G. fossarum* reached 2 μg g^{-1} gammarid dw, which is less than the toxic threshold of 8 μg g^{-1} gammarid dw previously reported in *G. fossarum* (Arce Funck et al., 2013). Observed differences in toxicities between $AgNO_3$ and AgNPs are most likely due to the ratio of NPs to free ions, which has been shown to be an important factor for toxicity. Nanoparticles used in the current study have low dissolution rate below 6% (Mehennaoui et al., 2018a), which may explain the lower toxicity observed for AgNPs.

Acute waterborne exposure of *G. fossarum* to CIT-AgNPs and CIT-AuNPs 40 nm resulted in an uptake of AgNPs in the gills and AuNPs in membrane of intestinal caeca of AuNPs (Mehennaoui et al., 2018a, Fig. 5). It was supposed that the necessity of feeding in the present work may have a significant effect on the pattern of internal distribution of AgNPs and AuNPs. Hence, digestive tissue was used to assess the internal distribution of AgNPs and AuNPs within *G. fossarum*. Coloured sections of intestinal caeca of *G. fossarum* exposed to the highest concentration of AgNPs and AuNPs (5 μg L^{-1}), used for the analyses of the response of the digestive lysosomal system, were used for enhanced dark field hyperspectral microscopy on a Cytoviva® instrument. The aim was to localise internalised AgNPs and AuNPs within the tissue and maybe within the lysosomes if they were impacted. Results allowed the observation of the activation of the lysosomal system in exposed organisms both to AgNPs and AuNPs, which may indicate their presence in the intestinal tissue (Fig. 5). Bigger and more lysosomes were observed in gammarids exposed to CIT-AgNPs and PEG-AgNPs when compared to control, while, no clear coating effect was observed between CIT-AgNPs and PEG-AgNPs. Similarly, *G. fossarum* exposed to AuNPs presented more lysosomes and bigger ones when compared to non-exposed animals. However, a coating-dependent effect was highlighted as bigger lysosomes were observed in gammarids exposed to PEG-AuNPs than those exposed to CIT-AuNPs. Unfortunately, the coloration of the tissues appeared as a confounding factor making impossible the distinction between metallic NPs and biological material. Indeed, one of the characteristic of Cytoviva® enhanced darkfield hyperspectral microscopy is the ability to detect nanoparticles without any coloration of the tissue as shown in our previous study (Mehennaoui et al., 2018a) and in others, using different aquatic model organism such as *Daphnia magna*, *Mytillus galloprovincialis* and the nematode *Caenorhabditis elegans* (Bosch et al., 2018; Botha et al., 2016; Duroudier et al., 2019; Mehennaoui et al., 2018a). However, the non-detection of AgNPs and AuNPs in *G. fossarum* tissue could be explained by the low level of the exposure concentration of 5 μg L^{-1} that could be under the detection of the Cytoviva®. Moreover, the activation of the lysosomal system may indicate a partial internal dissolution of AgNPs and AuNPs due to the acidic properties of the lysosomes (Lacave et al., 2020; Rocha et al., 2015). Although Cytoviva® is a good and powerful technique; it can only detect NPs and not the ions.

Gammarus fossarum exposed to AgNPs and AuNPs presented a more developed DLS compared to non-exposed organisms. These results are in agreement with those observed in other studies reporting the activation of the lysosomal system in other invertebrate species (Guerlet et al., 2010; Minguez et al., 2009) and fish (Lacave et al., 2020) exposed to different contaminants. In aquatic invertebrates, metals in both ions and NPs forms are known to activate the lysosomal system (Schultz et al., 2015) through an increased exocytosis of enlarged lysosomes in association with the synthesis of new ones (Guerlet et al., 2006; Marigómez et al., 1996) which correspond to our observation in the present study indicating a general stress response. However, very few studies investigated the impacts of NPs on the lysosomal system of gammarids. To our best knowledge, only one study has assessed the effects of cerium nanoparticles (CeO_2 NPs) on *G. roeseli* (Garaud et al., 2015). Cerium nanoparticles impact the lysosomal system of *G. roeseli* as smaller and less numerous lysosomes were observed when organisms were exposed to up to 100 μg L^{-1} d^{-1} of CeO_2 NPs for 4 days (Garaud et al., 2015). The most frequent response of the DLS is the enlargement of the lysosome which is in agreement with our results and with other previous studies (Guerlet et al., 2010). Two mechanisms could then be involved in the lysosome enlargement, an autophagic process responsible for the break of macromolecules (e.g. fats) into lower molecular weight compounds that are then used to build new cell materials through the cell's own lysosomal machinery (Moore and Halton, 1973), or a process of

General stress		DNA damage and repair			Lysosomes	Osmoregulation		Respiration	
GST	*HSP90*	*GAPDH*	*Gadd45*	*Cjun*	*CathL*	*Ca^{2+}ATPase*	*$Na^{+}K^{+}$ATPase*	*HEM*	*Cox1*
1 ± 0.34	1 ± 0.24	1 ± 0.2	1 ± 0.1	1 ± 0.24	1 ± 0.38	1 ± 0.3	1 ± 0.28	1 ± 0.24	1 ± 0.52
1.5 ± 0.42	1.07 ± 0.32	0.77 ± 0.16	1.04 ± 0.1	1.37 ± 0.22	**1.54 ± 0.7**	0.89 ± 0.88	1.13 ± 0.16	0.95 ± 0.08	1.07 ± 0.28
1 ± 0.44	1 ± 0.26	1 ± 0.2	1 ± 0.24	1 ± 0.52	1 ± 0.46	1 ± 0.2	1 ± 0.26	1 ± 0.28	1 ± 0.5
0.71 ± 0.3	1.33 ± 0.16	0.89 ± 0.08	1.15 ± 0.16	1.18 ± 0.4	0.61 ± 0.34	1.07 ± 0.3	**1.39 ± 0.3**	0.79 ± 0.08	1.11 ± 0.2
0.86 ± 0.32	0.93 ± 0.22	0.91 ± 0.14	1.06 ± 0.38	1.09 ± 0.4	0.76 ± 0.32	1.1 ± 0.36	**1.55 ± 0.32**	0.89 ± 0.14	1.4 ± 0.8
0.84 ± 0.16	1.09 ± 0.14	1.03 ± 0.3	1.27 ± 0.06	1.47 ± 0.44	0.74 ± 0.26	1.11 ± 0.08	**1.49 ± 0.16**	0.97 ± 0.3	**1.51 ± 0.6**
0.81 ± 0.24	1.42 ± 0.16	0.82 ± 0.22	1.26 ± 0.64	1.28 ± 0.14	0.69 ± 0.22	1.12 ± 0.06	**1.53 ± 0.24**	0.68 ± 0.22	0.97 ± 0.86
1 ± 0.26	1 ± 0.22	1 ± 0.18	1 ± 0.48	1 ± 0.14	1 ± 0.3	1 ± 0.1	1 ± 0.26	1 ± 0.18	1 ± 0.78
1.02 ± 0.18	0.66 ± 0.32	0.91 ± 0.22	0.89 ± 0.7	1.05 ± 0.26	1.09 ± 0.46	0.97 ± 0.12	0.95 ± 0.18	0.83 ± 0.22	0.68 ± 0.3
0.83 ± 0.28	0.86 ± 0.24	1.11 ± 0.08	1.15 ± 0.56	1.43 ± 0.54	0.88 ± 0.32	0.89 ± 0.12	0.81 ± 0.28	1.18 ± 0.08	0.97 ± 0.72
0.87 ± 0.08	0.69 ± 0.16	1 ± 0.28	0.81 ± 0.36	0.83 ± 0.3	0.82 ± 0.18	0.79 ± 0.14	0.66 ± 0.0	1.23 ± 0.28	1.12 ± 0.3
1.13 ± 0.28	0.96 ± 0.16	0.68 ± 0.34	1.06 ± 1.08	1.27 ± 0.34	1.31 ± 0.54	0.88 ± 0.14	0.8 ± 0.28	0.92 ± 0.34	1.15 ± 1.12

apoptosis involving the degradation of cells into apoptotic bodies and their phagocytosis by surrounding cells (Pipe and Moore, 1985). The increase of the volume and the surface of the lysosomal system could also be linked to the sequestration/detoxification process of xenobiotics in addition to the damaged cellular compounds (Garaud et al., 2015; Giambérini and Cajaraville, 2005b; Guerlet et al., 2010).

A set of stress-related genes was used in order to investigate the effects of AgNPs and AuNPs 40 nm at the molecular level (Mehennaoui et al., 2018a). Both concentrations (0.5 and 5 μg L^{-1}) of PEG-AgNPs 40 nm led to an up-regulation of *catalase* and *chitinase* and CIT-AgNPs and PEG-AgNPs 40 nm led to an up-regulation of *$Na^{+}K^{+}ATPase$*. The highest concentration of CIT and PEG-AuNPs 40 nm (5 μg L^{-1}) led to an increase of *CuZnSOD* gene expression. One previous study reported an over-expression of *SOD* and catalase in *G. fossarum* exposed for 48 h to 4.56 mg L^{-1} of positively charged AuNPs 10 nm (Baudrimont et al., 2017). This was linked to up-regulation of antioxidant defence to the increase of the number of mitochondria, observed via induction of *16S* gene, as these mechanisms require energy (Baudrimont et al., 2017). As previously described, the acute toxicity of Ag is exerted through the inhibition of $Na^{+}K^{+}$ATPase activity. A prolonged exposure may have led to an adaptive strategy leading to the up-regulation of *$Na^{+}K^{+}ATPase$* in order to offset the inhibition of the enzymatic activity. These results highlight the differences or evolution of gene expression responses observed after an acute waterborne exposure of *G. fossarum* to AgNPs and AuNPs (Mehennaoui et al., 2018a) and chronic exposure in the presence of food to the same particles.

No significant effects of AgNPs or AuNPs on concentrations of haemolymphatic ions, Na^{+} and Cl^{-}, were observed. As described above, the internal Ag concentration reached 2 μg g^{-1} gammarids d.w. indicating a potential lower Ag uptake through the gills. The presence of food during exposure may have decreased the bioavailability of Ag, leading to the formation of different complexes with biomolecules, thus in turn making Ag less toxic or favouring a different uptake route (Mann et al., 2004; Webb and Wood, 1998). The absence of effects on concentrations of

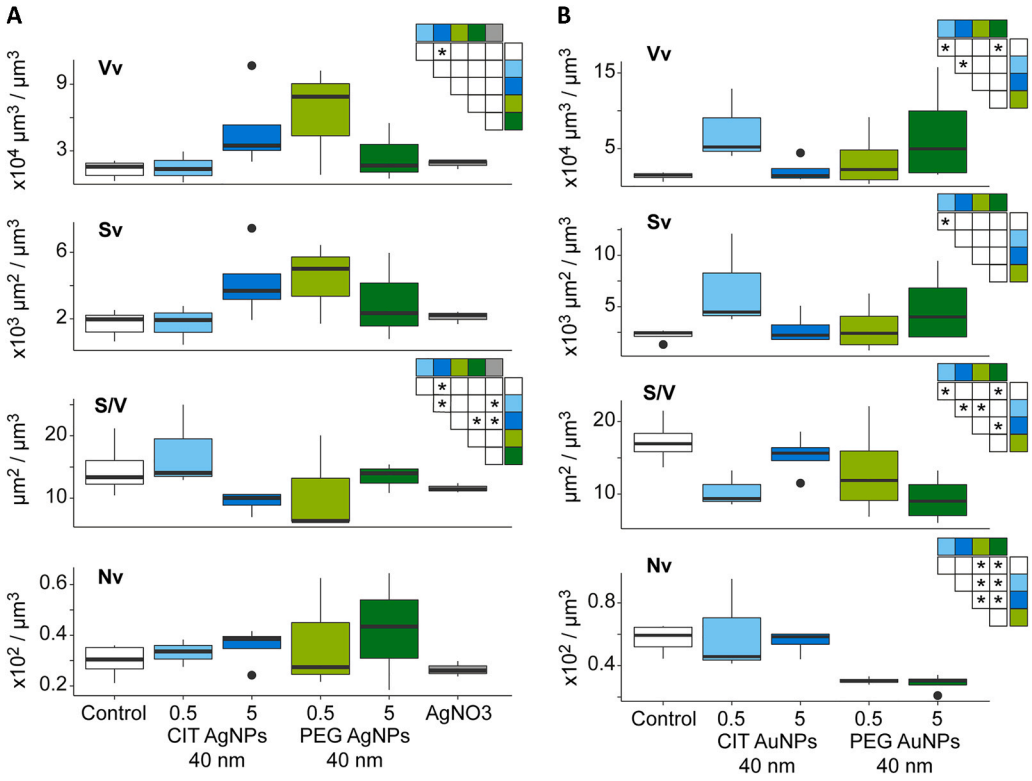

Fig. 1. Structural changes of lysosomal system in *G. fossarum* exposed for 15 days to: A: CIT and PEG-AgNPs 40 nm and B: CIT and PEG-AuNPs 40 nm. Boxplots show median values, quartiles (hinges), extremes (whiskers) and outliers (dots). Four stereological parameters of lysosome are calculated: the volume density (Vv = VL/VC; $x10^4$ $\mu m^3/\mu m^3$), the surface density (Sv = SL/VC; $x10^3$ $\mu m^2/\mu m^3$), the surface to volume ratio (S/V = SL/VL, $\mu m^2/\mu m^2$ corresponding to the inverse of lysosome size) and the numerical density (Nv = NL/VC; $x10^2/\mu m^3$). C corresponds to digestive cell cytoplasm; L corresponds to lysosomes, N to numbers, S to surface and V to volume. Significant differences are indicated by stars in the matrix.

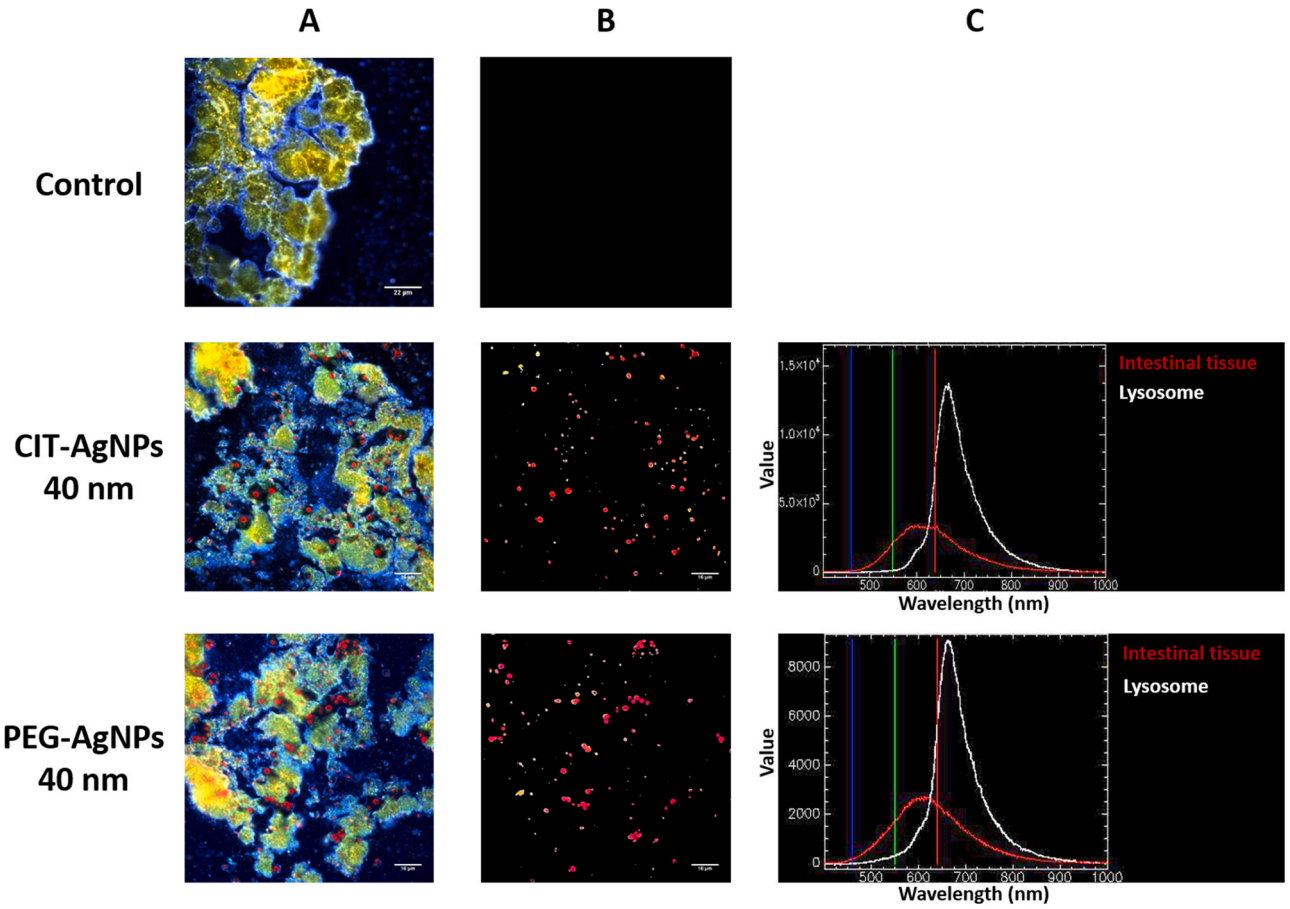

Fig. 2. (A) Coloured 8 μm section of intestinal caeca of *G. fossarum* observed under hyperspectral microscope. Scale bar is 22 μm for Control and 16 μm for CIT-AgNPs and PEG-AgNPs. (B) Lysosomes detected in *G. fossarum* intestinal caeca viewed with Cytoviva (60x oil immersion magnification). Scale bar is 16 μm. (C) Spectral profile of the intestinal caeca tissue (white) and lysosome (red). Animals were exposed for 15 days to 5 μg L^{-1} of CIT-AgNPs 40 nm and PEG-AgNPs 40 nm in Volvic water in presence of food. (For interpretation of the references to colour in this figure legend, the reader is referred to the web version of this article.)

haemolymphatic ions may indicate a lower presence of AgNPs in *G. fossarum* gills which are known as one of the main uptake route of contaminants as they are in direct contact with the external environment (Mann et al., 2004). The presence of food could also modify the uptake route of AgNPs and AuNPs. Indeed, it could be suggested that AgNPs and AuNPs complexed with the food could be eliminated with faeces without crossing intestinal barrier and reaching the circulatory system. Gold nanoparticles were observed in the gut of *D. magna* after direct exposure and were not eliminated while the presence of food during the experiment resulted in their elimination (Botha et al., 2016). Other studies reported an adsorption of AuNPs on algae surface which led to their ingestion by *D. magna* followed by a rapid elimination from the gut (Khan et al., 2014; Volland et al., 2015; Wray and Klaine, 2015). Gammarids exposed to metallic contaminants are usually described to exhibit an iono/osmotic disruption including changes in the Na^+K^+ATPase activity, ions influx and gills surface permeability (Lignot et al., 2000). Osmoregulation impairment can therefore be noticed by an impact on haemolymphatic Na^+ and Cl^- concentrations which represent 90% of the osmotic pressure in gammarids (Mantel and Farmer, 1983). It is also known that an acute exposure to Ag generally lead to the inhibition of Na^+ uptake through the inhibition of Na^+K^+ATPase activity (Bianchini and Wood, 2003, 2002; Bury et al., 2002; Grosell et al., 2002; Webb and Wood, 1998). This mechanism was previously observed in *G. fossarum* exposed to $AgNO_3$ and AgNPs 23 nm for up to 96 h (Arce Funck et al., 2013; Mehennaoui et al., 2016).

Movement of *G. fossarum* was significantly reduced following exposure to CIT and PEG-AgNPs 40 nm for 15 days. This result is in accordance with our previous finding where a decrease in locomotor activity was observed in *G. fossarum* exposed for 72 h to AgNPs 23 nm (Mehennaoui et al., 2016). Similarly, a decrease in locomotor activity of *G. roeseli* exposed for 72 h to CIT-AgNPs 10 and 60 nm was observed (Andreï et al., 2016). A size-dependent effect on locomotion was reported as CIT-AgNPs 10 nm was more effective than CIT-AgNPs 60 nm (Andreï et al., 2016). The effects of CIT-AgNPs 10 nm was as strong as the effects observed for $AgNO_3$ (Andreï et al., 2016; Arce Funck et al., 2013). Therefore, it may be suggested that the readily taken up AgNPs dissolve internally and release Ag^+ ions that are more potent in inhibiting *G. fossarum* locomotor activity (Arce Funck et al., 2013; Mehennaoui et al., 2016). The effects on locomotion could also be linked to sensorial disruption linked to the adsorption of AgNPs and AuNPs on the carapace of *G. fossarum* as observed in our previous study (Mehennaoui et al., 2018a) and which is consistent with the significant effect of AgNPs on the expression of *chitinase*. The lowest concentrations of both AgNPs and AuNPs 40 nm (0.5 μg L^{-1}) led to a higher reduction of locomotor activity of *G. fossarum* when compared to the highest ones (5 μg L^{-1}), although the differences were not significant in gammarids exposed to PEG-AuNPs 40 nm. A first hypothesis is that at the highest concentration the adsorption of AgNPs and AuNPs on the particulate matter from the medium and food debris is more important, leading to the formation of bigger aggregates. These aggregates may have less impacts on the locomotion as they behave as bigger NPs described to have less effects on locomotion (Andreï et al., 2016). Another hypothesis is the higher concentrations of NPs might tend to quickly reach a maximum level of uptake and adsorption leading to a potential acclimation of the exposed organisms (Bossus et al., 2014). The decrease in locomotor activity could also be a result of an energy reallocation in favour of defence

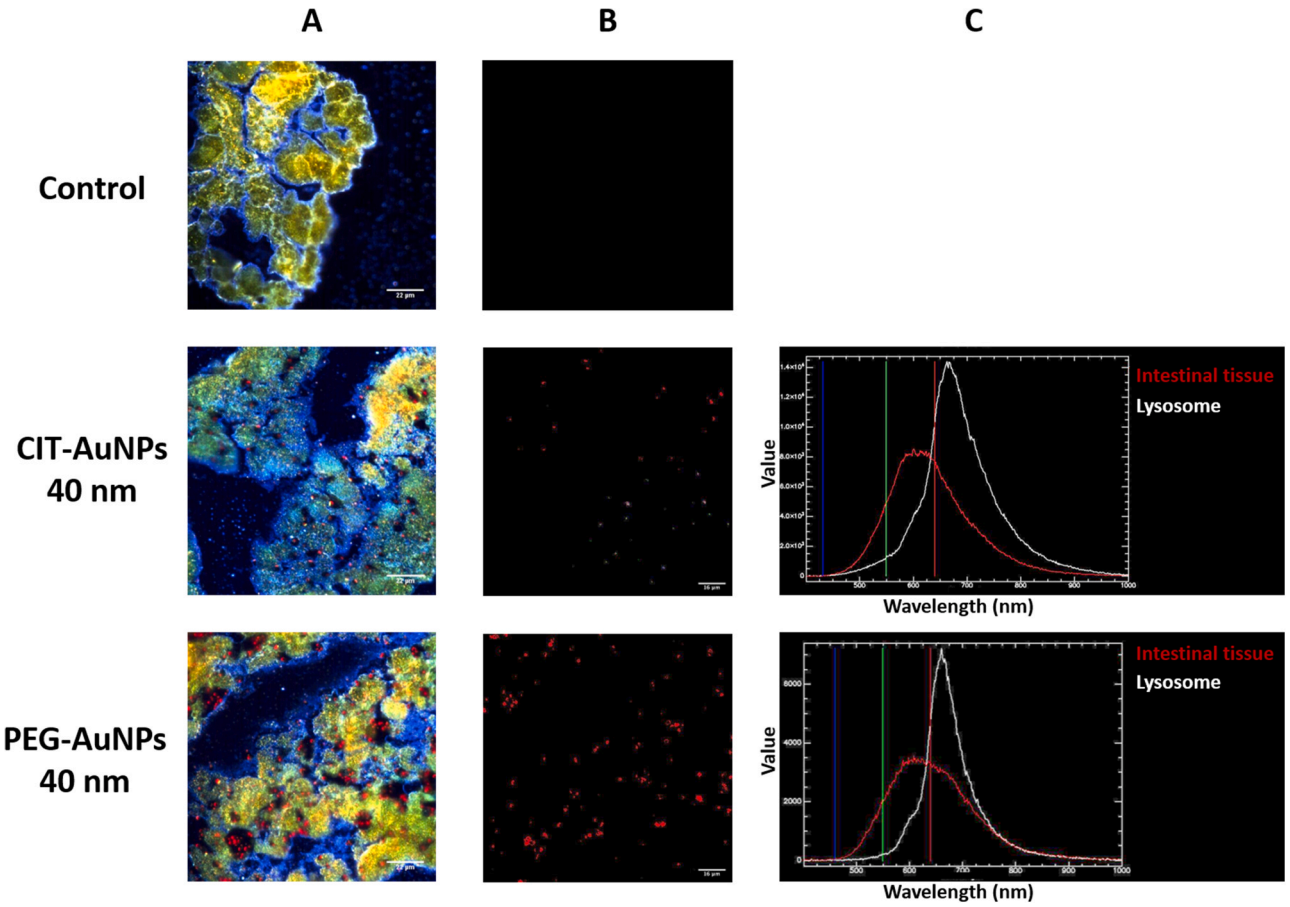

Fig. 3. (A) Coloured 8 μm section of intestinal caeca of *G. fossarum* observed under hyperspectral microscope. Scale bar is 22 μm. (B) Lysosomes detected in *G. fossarum* intestinal caeca viewed with Cytoviva (60x oil immersion magnification). Scale bar is 16 μm. (C) Spectral profile of the intestinal caeca tissue (white) and lysosome (red). Animals were exposed for 15 days to 5 μg L^{-1} of CIT-AuNPs 40 nm and PEG-AuNPs 40 nm in Volvic water in presence of food. (For interpretation of the references to colour in this figure legend, the reader is referred to the web version of this article.)

mechanisms (Fig. 5). Indeed, an increase in the internal concentrations of metals or NPs usually lead individuals to invest their energy in highly energy consuming mechanisms such as detoxification, homoeostasis maintenance (iono/osmoregulation, activation of lysosomal system) or cellular repairing process (Arce Funck et al., 2013; Vellinger et al., 2013, Fig. 5). This study highlights once more the great sensitivity of behavioural responses that are fast, simple to perform, cheap and non-invasive biological endpoints that can highlight sub-lethal effects of contaminants at very low concentration (0.5 μg L^{-1}). Behavioural responses allow linking responses observed at the physiological level to potential effects at the individual, population and community levels regarding the central position of *G. fossarum* in aquatic ecosystems. Indeed, an impairment of locomotion may have consequent effects on the fitness of an organism and lead to "ecological death" (Scott and Sloman, 2004, Fig. 5).

5. Conclusion

The present study allowed obtaining first insights on key mechanisms of sub-chronic effects of AgNPs and AuNPs and allowed the identification of a potential AOP for AgNPs and AuNPs toxicity on *G. fossarum* (Fig. 5). Gene expression, response of the digestive lysosomal system and locomotion appeared to be relevant biological endpoints as they allow the detection of sub-lethal effects of AgNPs and AuNPs at very low concentration (0.5 μg L^{-1}). Similarly to the acute exposure (Mehennaoui et al., 2018a), chemical composition of AgNPs and AuNPs appear as the main factor influencing the fate and effects of these compounds on *G. fossarum*. Indeed, different patterns of internal uptake were observed as AgNPs led to high Ag concentration in exposed organisms compared to AuNPs. Different genes were impacted when gammarids were exposed either to AgNPs or to AuNPs and AgNPs had a higher impact on locomotor activity than AuNPs. Gene expression results may allow an early prediction of effects of AgNPs and AuNPs on *G. fossarum*. Digestive lysosomal system changes as a general stress response indicate the general health status of *G. fossarum*. Locomotion may predict effects at the population and community level regarding the central position of *G. fossarum* in aquatic ecosystems (Fig. 5).

CRediT authorship contribution statement

K.M. conceived, designed and performed the experiments, prepared tables and figures and wrote the manuscript. L.M. performed lysosome

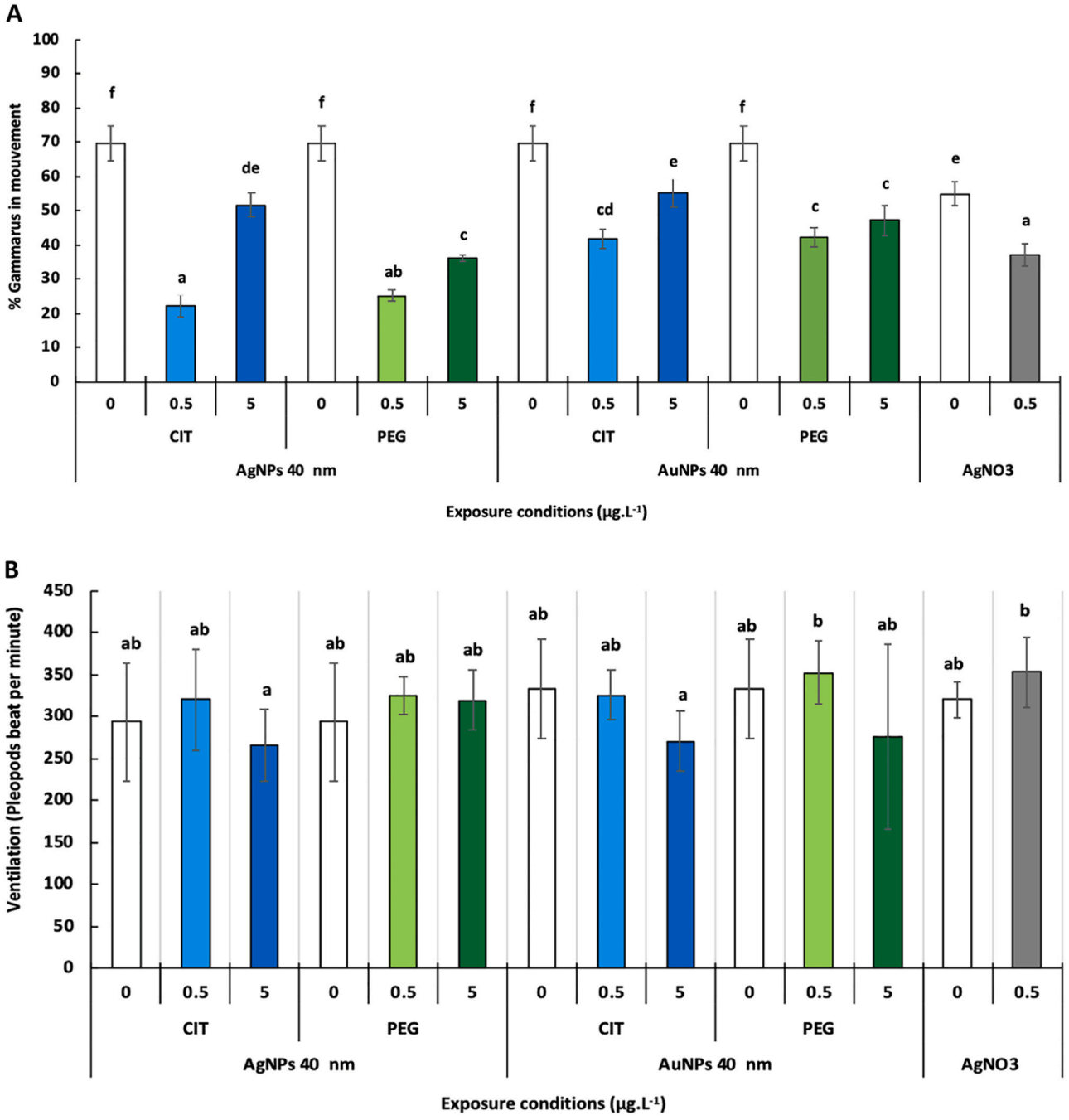

Fig. 4. Behavioural responses of *G. fossarum* exposed for 15 days to CIT and PEG-AgNPs and AuNPs 40 nm. (A) Locomotor activity (mean percentage of moving *G. fossarum* ± SD) and (B) Ventilation (mean pleopods beat frequency ± SD). Different letters (a–f) indicate significant differences (one-way ANOVA + Tukey HSD post hoc test at $P < 0.05$ level of significance, n = 10).

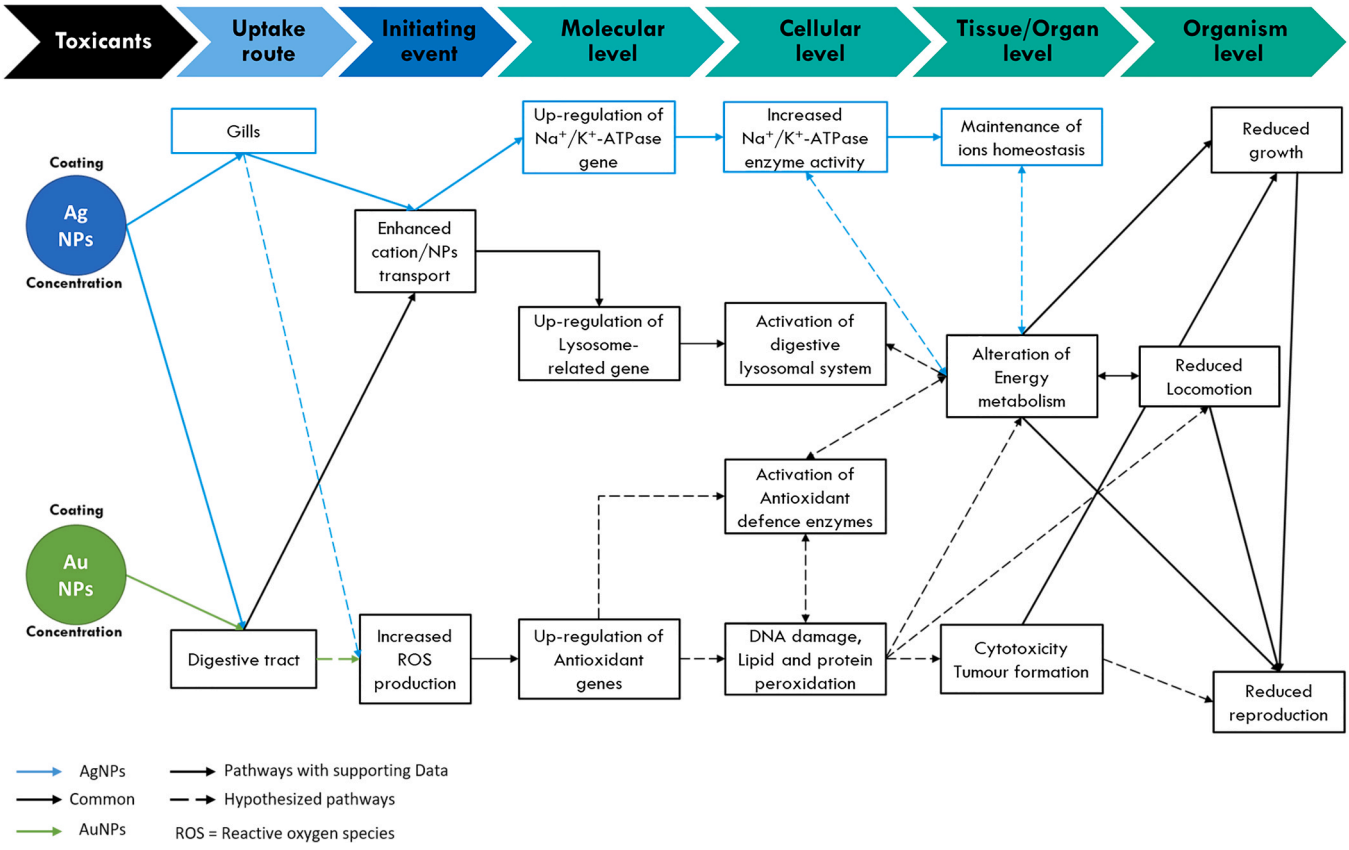

Fig. 5. Adverse outcome pathway (AOP) for AgNPs and AuNPs toxicity to *G. fossarum*. Blue lines indicate AgNPs specific pathways. Green line indicates AuNPs specific pathways. Black lines indicate pathways common to both AgNPs and AuNPs. Solid arrows represent pathways with supporting data. Dashed arrows indicate hypothetical pathways. (For interpretation of the references to colour in this figure legend, the reader is referred to the web version of this article.)

measurements, analysed data and prepared lysosome figures. K.M and S. C. analysed the data. S.C., T.S., A.C.G., L.G. coordinated manuscript revision; read and provided helpful discussions and approved the final discussion.

Declaration of Competing Interest

The authors declare that they have no known competing financial interests or personal relationships that could have appeared to influence the work reported in this paper.

Acknowledgments

This work was supported by National Research Fund, Luxembourg (AFR-PhD-9229040). The authors are thankful to S. Contal and A. Lorette for technical support, P. Rouselle, C. Guignard and J. Ziebel for chemical analyses.

Appendix A. Supporting information

Supplementary data associated with this article can be found in the online version at doi:10.1016/j.ecoenv.2020.111775.

References

Abbas, Q., Yousaf, B., Amina, Ali, M.U., Munir, M.A.M., El-Naggar, A., Rinklebe, J., Naushad, M., 2020. Transformation pathways and fate of engineered nanoparticles (ENPs) in distinct interactive environmental compartments: a review. Environ. Int. 138, 105646 https://doi.org/10.1016/j.envint.2020.105646.

Andreï, J., Pain-Devin, S., Felten, V., Devin, S., Giambérini, L., Mehennaoui, K., Cambier, S., Gutleb, A.C., Guérold, F., 2016. Silver nanoparticles impact the functional role of Gammarus roeseli (Crustacea Amphipoda). Environ. Pollut. 208 (Part B), 608–618. https://doi.org/10.1016/j.envpol.2015.10.036.

Arce Funck, J., Danger, M., Gismondi, E., Cossu-Leguille, C., Guérold, F., Felten, V., 2013. Behavioural and physiological responses of Gammarus fossarum (Crustacea Amphipoda) exposed to silver. Aquat. Toxicol. 142–143, 73–84. https://doi.org/10.1016/j.aquatox.2013.07.012.

Artal, M.C., Pereira, K.D., Luchessi, A.D., Okura, V.K., Henry, T.B., Marques-Souza, H., de Aragão Umbuzeiro, G., 2020. Transcriptome analysis in Parhyale hawaiensis reveal sex-specific responses to AgNP and AgCl exposure. Environ. Pollut. 260, 113963 https://doi.org/10.1016/j.envpol.2020.113963.

Bai, C., Tang, M., 2020. Toxicological study of metal and metal oxide nanoparticles in zebrafish. J. Appl. Toxicol. 40, 37–63. https://doi.org/10.1002/jat.3910.

Batista, D., Pascoal, C., Cássio, F., 2017. How do physicochemical properties influence the toxicity of silver nanoparticles on freshwater decomposers of plant litter in streams? Ecotoxicol. Environ. Saf. 140, 148–155. https://doi.org/10.1016/j.ecoenv.2017.02.039.

Baudrimont, M., Andrei, J., Mornet, S., Gonzalez, P., Mesmer-Dudons, N., Gourves, P.-Y., Jaffal, A., Dedourge-Geffard, O., Geffard, A., Geffard, O., Garric, J., Feurtet-Mazel, A., 2017. Trophic transfer and effects of gold nanoparticles (AuNPs) in Gammarus fossarum from contaminated periphytic biofilm. Environ. Sci. Pollut. Res. https://doi.org/10.1007/s11356-017-8400-3.

Behr, M., Legay, S., Hausman, J.-F., Guerriero, G., 2015. Analysis of cell wall-related genes in organs of medicago sativa L. under different abiotic stresses. Int. J. Mol. Sci. 16, 16104–16124. https://doi.org/10.3390/ijms160716104.

Bianchini, A., Wood, C.M., 2003. Mechanism of acute silver toxicity in Daphnia magna. Environ. Toxicol. Chem. 22, 1361–1367. https://doi.org/10.1002/etc.5620220624.

Bianchini, A., Wood, C.M., 2002. Physiological effects of chronic silver exposure in Daphnia magna. Comp. Biochem. Physiol. Toxicol. Pharmacol. CBP 133, 137–145.

Blinova, I., Niskanen, J., Kajankari, P., Kanarbik, L., Käkinen, A., Tenhu, H., Penttinen, O.-P., Kahru, A., 2012. Toxicity of two types of silver nanoparticles to aquatic crustaceans Daphnia magna and Thamnocephalus platyurus. Environ. Sci. Pollut. Res. 1–8. https://doi.org/10.1007/s11356-012-1290-5.

Bosch, S., Botha, T.L., Jordaan, A., Maboeta, M., Wepener, V., 2018. Sublethal effects of ionic and nanogold on the nematode Caenorhabditis elegans. J. Toxicol. 2018, 1–11. https://doi.org/10.1155/2018/6218193.

Bossus, M.C., Guler, Y.Z., Short, S.J., Morrison, E.R., Ford, A.T., 2014. Behavioural and transcriptional changes in the amphipod Echinogammarus marinus exposed to two antidepressants, fluoxetine and sertraline. Aquat. Toxicol. Antidepressants Aquat. Environ. 151, 46–56. https://doi.org/10.1016/j.aquatox.2013.11.025.

Botha, T.L., Boodhia, K., Wepener, V., 2016. Adsorption, uptake and distribution of gold nanoparticles in Daphnia magna following long term exposure. Aquat. Toxicol. 170, 104–111. https://doi.org/10.1016/j.aquatox.2015.11.022.

Buffet, P.-E., Pan, J.-F., Poirier, L., Amiard-Triquet, C., Amiard, J.-C., Gaudin, P., Faverney, C.R., Guibbolini, M., Gilliland, D., Valsami-Jones, E., Mouneyrac, C., 2013. Biochemical and behavioural responses of the endobenthic bivalve Scrobicularia plana to silver nanoparticles in seawater and microalgal food. Ecotoxicol. Environ. Saf. 89, 117–124. https://doi.org/10.1016/j.ecoenv.2012.11.019.

Bury, N.R., Shaw, J., Glover, C., Hogstrand, C., 2002. Derivation of a toxicity-based model to predict how water chemistry influences silver toxicity to invertebrates. Comp. Biochem. Physiol. Part C Toxicol. Pharmacol. 133, 259–270. https://doi.org/10.1016/S1532-0456(02)00096-0.

Cajaraville, M.P., Marigómez, J.A., Angulo, E., 1991. Automated measurement of lysosomal structure alterations in oocytes of mussels exposed to petroleum hydrocarbons. Arch. Environ. Contam. Toxicol. 21, 395–400. https://doi.org/10.1007/BF01060362.

Cambier, S., Røgeberg, M., Georgantzopoulou, A., Serchi, T., Karlsson, C., Verhaegen, S., Iversen, T.-G., Guignard, C., Kruszewski, M., Hoffmann, L., Audinot, J.-N., Ropstad, E., Gutleb, A.C., 2018. Fate and effects of silver nanoparticles on early life-stage development of zebrafish (Danio rerio) in comparison to silver nitrate. Sci. Total Environ. 610, 972–982. https://doi.org/10.1016/j.scitotenv.2017.08.115.

Clark, N.J., Clough, R., Boyle, D., Handy, R.D., 2019. Development of a suitable detection method for silver nanoparticles in fish tissue using single particle ICP-MS. Environ. Sci. Nano 6, 3388–3400. https://doi.org/10.1039/C9EN00547A.

Croteau, M.-N., Misra, S.K., Luoma, S.N., Valsami-Jones, E., 2011. Silver bioaccumulation dynamics in a freshwater invertebrate after aqueous and dietary exposures to nanosized and ionic Ag. Environ. Sci. Technol. 45, 6600–6607. https://doi.org/10.1021/es200880c.

Dedourge-Geffard, O., Palais, F., Biagianti-Risbourg, S., Geffard, O., Geffard, A., 2009. Effects of metals on feeding rate and digestive enzymes in Gammarus fossarum: an in situ experiment. Chemosphere 77, 1569–1576. https://doi.org/10.1016/j.chemosphere.2009.09.042.

Dohet, A., Ector, L., Cauchie, H.-M., Hoffmann, L., 2008. Identification of benthic invertebrate and diatom indicator taxa that distinguish different stream types as well as degraded from reference conditions in Luxembourg. Anim. Biol. 58, 419–472. https://doi.org/10.1163/157075608×383719.

Duroudier, N., Cardoso, C., Mehennaoui, K., Mikolaczyk, M., Schäfer, J., Gutleb, A.C., Giamberini, L., Bebianno, M.J., Bilbao, E., Cajaraville, M.P., 2019. Changes in protein expression in mussels Mytilus galloprovincialis dietarily exposed to PVP/PEI coated silver nanoparticles at different seasons. Aquat. Toxicol. 210, 56–68. https://doi.org/10.1016/j.aquatox.2019.02.010.

Farkas, J., Christian, P., Gallego-Urrea, J.A., Roos, N., Hassellöv, M., Tollefsen, K.E., Thomas, K.V., 2011. Uptake and effects of manufactured silver nanoparticles in rainbow trout (Oncorhynchus mykiss) gill cells. Aquat. Toxicol. 101, 117–125. https://doi.org/10.1016/j.aquatox.2010.09.010.

Farré, M., Gajda-Schrantz, K., Kantiani, L., Barceló, D., 2008. Ecotoxicity and analysis of nanomaterials in the aquatic environment. Anal. Bioanal. Chem. 393, 81–95. https://doi.org/10.1007/s00216-008-2458-1.

Felten, V., Charmantier, G., Mons, R., Geffard, A., Rousselle, P., Coquery, M., Garric, J., Geffard, O., 2008. Physiological and behavioural responses of Gammarus pulex (Crustacea: Amphipoda) exposed to cadmium. Aquat. Toxicol. 86, 413–425. https://doi.org/10.1016/j.aquatox.2007.12.002.

Forrow, D.M., Maltby, L., 2000. Toward a mechanistic understanding of contaminant-induced changes in detritus processing in streams: Direct and indirect effects on detritivore feeding. Environ. Toxicol. Chem. 19, 2100–2106. https://doi.org/10.1002/etc.5620190820.

Gaiser, B.K., Biswas, A., Rosenkranz, P., Jepson, M.A., Lead, J.R., Stone, V., Tyler, C.R., Fernandes, T.F., 2011. Effects of silver and cerium dioxide micro- and nano-sized particles on Daphnia magna. J. Environ. Monit. 13, 1227–1235. https://doi.org/10.1039/C1EM10060B.

Galhano, V., Hartmann, S., Monteiro, M.S., Zeumer, R., Mozhayeva, D., Steinhoff, B., Müller, K., Prenzel, K., Kunze, J., Kuhnert, K.-D., Schönherr, H., Engelhard, C., Schlechtriem, C., Loureiro, S., Soares, A.M.V.M., Witte, K., Lopes, I., 2020. Impact of wastewater-borne nanoparticles of silver and titanium dioxide on the swimming behaviour and biochemical markers of Daphnia magna: an integrated approach. Aquat. Toxicol. 220, 105404 https://doi.org/10.1016/j.aquatox.2020.105404.

Gallego-Urrea, J.A., Tuoriniemi, J., Hassellöv, M., 2011. Applications of particle-tracking analysis to the determination of size distributions and concentrations of nanoparticles in environmental, biological and food samples. TrAC Trends Anal. Chem. 30, 473–483. https://doi.org/10.1016/j.trac.2011.01.005.

Garaud, Trapp, J., Devin, S., Cossu-Leguille, C., Pain-Devin, S., Felten, V., Giamberini, L., 2015. Multibiomarker assessment of cerium dioxide nanoparticle (nCeO2) sublethal effects on two freshwater invertebrates, Dreissena polymorpha and Gammarus roeseli. Aquat. Toxicol. 158, 63–74. https://doi.org/10.1016/j.aquatox.2014.11.004.

García-Alonso, J., Rodriguez-Sanchez, N., Misra, S.K., Valsami-Jones, E., Croteau, M.-N., Luoma, S.N., Rainbow, P.S., 2014. Toxicity and accumulation of silver nanoparticles during development of the marine polychaete Platynereis dumerilii. Sci. Total Environ. 476–477, 688–695. https://doi.org/10.1016/j.scitotenv.2014.01.039.

García-Cambero, J.P., Núñez García, M., López, G.D., Herranz, A.L., Cuevas, L., Pérez-Pastrana, E., Cuadal, J.S., Castelltort, M.R., Calvo, A.C., 2013. Converging hazard assessment of gold nanoparticles to aquatic organisms. Chemosphere 93, 1194–1200. https://doi.org/10.1016/j.chemosphere.2013.06.074.

Giambérini, L., Cajaraville, M.P., 2005a. Lysosomal responses in the digestive gland of the freshwater mussel, Dreissena polymorpha, experimentally exposed to cadmium. Environ. Res. 98, 210–214. https://doi.org/10.1016/j.envres.2004.11.003.

Giambérini, L., Cajaraville, M.P., 2005b. Lysosomal responses in the digestive gland of the freshwater mussel, Dreissena polymorpha, experimentally exposed to cadmium. Environ. Res. 98, 210–214. https://doi.org/10.1016/j.envres.2004.11.003.

Gottschalk, F., Sun, T., Nowack, B., 2013. Environmental concentrations of engineered nanomaterials: review of modeling and analytical studies. Environ. Pollut. 181, 287–300. https://doi.org/10.1016/j.envpol.2013.06.003.

Grosell, M., Nielsen, C., Bianchini, A., 2002. Sodium turnover rate determines sensitivity to acute copper and silver exposure in freshwater animals. Comp. Biochem. Physiol. Part C Toxicol. Pharmacol. 133, 287–303. https://doi.org/10.1016/S1532-0456(02)00085-6.

Guerlet, E., Ledy, K., Giambérini, L., 2006. Field application of a set of cellular biomarkers in the digestive gland of the freshwater snail Radix peregra (Gastropoda, Pulmonata). Aquat. Toxicol. 77, 19–32. https://doi.org/10.1016/j.aquatox.2005.10.012.

Guerlet, E., Vasseur, P., Giambérini, L., 2010. Spatial and temporal variations of biological responses to environmental pollution in the freshwater zebra mussel. Ecotoxicol. Environ. Saf. 73, 1170–1181. https://doi.org/10.1016/j.ecoenv.2010.05.009.

Hole, P., Sillence, K., Hannell, C., Maguire, C.M., Roesslein, M., Suarez, G., Capracotta, S., Magdolenova, Z., Horev-Azaria, L., Dybowska, A., Cooke, L., Haase, A., Contal, S., Manø, S., Vennemann, A., Sauvain, J.-J., Staunton, K.C., Anguissola, S., Luch, A., Dusinska, M., Korenstein, R., Gutleb, A.C., Wiemann, M., Prina-Mello, A., Riediker, M., Wick, P., 2013. Interlaboratory comparison of size measurements on nanoparticles using nanoparticle tracking analysis (NTA). J. Nanopart. Res. 15, 1–12. https://doi.org/10.1007/s11051-013-2101-8.

Janetzky, W., 1994. Distribution of the genus Gammarus (Amphipoda: Gammaridae) in the River Hunte and its tributaries (Lower Saxony, northern Germany). Hydrobiologia 294, 23–34. https://doi.org/10.1007/BF00017622.

Kaegi, R., Sinnet, B., Zuleeg, S., Hagendorfer, H., Mueller, E., Vonbank, R., Boller, M., Burkhardt, M., 2010. Release of silver nanoparticles from outdoor facades. Environ. Pollut. 158, 2900–2905. https://doi.org/10.1016/j.envpol.2010.06.009.

Kelly, D.W., Dick, J.T.A., Montgomery, W.I., 2002. The functional role of Gammarus (Crustacea, Amphipoda): shredders, predators, or both? Hydrobiologia 485, 199–203. https://doi.org/10.1023/A:1021370405349.

Khan, F.R., Kennaway, G.M., Croteau, M.-N., Dybowska, A., Smith, B.D., Nogueira, A.J.A., Rainbow, P.S., Luoma, S.N., Valsami-Jones, E., 2014. In vivo retention of ingested Au NPs by Daphnia magna: no evidence for trans-epithelial alimentary uptake. Chemosphere 100, 97–104. https://doi.org/10.1016/j.chemosphere.2013.12.051.

Klaine, S.J., Alvarez, P.J.J., Batley, G.E., Fernandes, T.F., Handy, R.D., Lyon, D.Y., Mahendra, S., McLaughlin, M.J., Lead, J.R., 2008. Nanomaterials in the environment: behavior, fate, bioavailability, and effects. Environ. Toxicol. Chem. 27, 1825–1851. https://doi.org/10.1897/08-090.1.

Lacave, J.M., Bilbao, E., Gilliland, D., Mura, F., Dini, L., Cajaraville, M.P., Orbea, A., 2020. Bioaccumulation, cellular and molecular effects in adult zebrafish after exposure to cadmium sulphide nanoparticles and to ionic cadmium. Chemosphere 238, 124588. https://doi.org/10.1016/j.chemosphere.2019.124588.

Lacaze, E., Geffard, O., Bony, S., Devaux, A., 2010. Genotoxicity assessment in the amphipod Gammarus fossarum by use of the alkaline Comet assay. Mutat. Res. Toxicol. Environ. Mutagen 700, 32–38. https://doi.org/10.1016/j.mrgentox.2010.04.025.

Ladewig, V., Jungmann, D., Köhler, H.-R., Schirling, M., Triebskorn, R., Nagel, R., 2006. Population structure and dynamics of Gammarus fossarum (Amphipoda) upstream and downstream from effluents of sewage treatment plants. Arch. Environ. Contam. Toxicol. 50, 370–383. https://doi.org/10.1007/s00244-005-7039-0.

Lapresta-Fernández, A., Fernández, A., Blasco, J., 2012. Nanoecotoxicity effects of engineered silver and gold nanoparticles in aquatic organisms. TrAC Trends Anal. Chem. 32, 40–59. https://doi.org/10.1016/j.trac.2011.09.007.

Legay, S., Guerriero, G., Deleruelle, A., Lateur, M., Evers, D., André, C.M., Hausman, J.-F., 2015. Apple russeting as seen through the RNA-seq lens: strong alterations in the exocarp cell wall. Plant Mol. Biol. 88, 21–40. https://doi.org/10.1007/s11103-015-0303-4.

Levard, C., Hotze, E.M., Lowry, G.V., Brown, G.E., 2012. Environmental transformations of silver nanoparticles: impact on stability and toxicity. Environ. Sci. Technol. 46, 6900–6914. https://doi.org/10.1021/es2037405.

Lignot, J.-H., Spanings-Pierrot, C., Charmantier, G., 2000. Osmoregulatory capacity as a tool in monitoring the physiological condition and the effect of stress in crustaceans. Aquaculture 191, 209–245. https://doi.org/10.1016/S0044-8486(00)00429-4.

Lüderwald, S., Schell, T., Newton, K., Salau, R., Seitz, F., Rosenfeldt, R.R., Dackermann, V., Metreveli, G., Schulz, R., Bundschuh, M., 2019. Exposure pathway dependent effects of titanium dioxide and silver nanoparticles on the benthic amphipod Gammarus fossarum. Aquat. Toxicol. 212, 47–53. https://doi.org/10.1016/j.aquatox.2019.04.016.

Luoma, S.N., Khan, F.R., Croteau, M.-N., 2014. Chapter 5 - Bioavailability and bioaccumulation of metal-based engineered nanomaterials in aquatic environments: concepts and processes. In: Lead, Jamie R., Valsami-Jones, Eugenia (Eds.), Frontiers of Nanoscience, Nanoscience and the Environment. Elsevier, pp. 157–193.

Luoma, S.N., Rainbow, P.S., 2005. Why is metal bioaccumulation so variable? Biodynamics as a unifying concept. Environ. Sci. Technol. 39, 1921–1931. https://doi.org/10.1021/es048947e.

Mackevica, A., Skjolding, L.M., Gergs, A., Palmqvist, A., Baun, A., 2015. Chronic toxicity of silver nanoparticles to Daphnia magna under different feeding conditions. Aquat. Toxicol. 161, 10–16. https://doi.org/10.1016/j.aquatox.2015.01.023.

MacNeil, C., Dick, J.T.A., Elwood, R.W., 1997. The trophic ecology of freshwater Gammarus Spp. (crustacea:amphipoda): problems and perspectives concerning the

functional feeding group concept. Biol. Rev. 72, 349–364. https://doi.org/10.1111/j.1469-185X.1997.tb00017.x.
Maguire, C.M., Sillence, K., Roesslein, M., Hannell, C., Suarez, G., Sauvain, J.-J., Capracotta, S., Contal, S., Cambier, S., El Yamani, N., Dusinska, M., Dybowska, A., Vennemann, A., Cooke, L., Haase, A., Luch, A., Wiemann, M., Gutleb, A., Korenstein, R., Riediker, M., Wick, P., Hole, P., Prina-Mello, A., 2017. Benchmark of nanoparticle tracking analysis on measuring nanoparticle sizing and concentration. J. Micro Nano-Manuf. 5 https://doi.org/10.1115/1.4037124.
Mann, R.M., Grosell, M., Bianchini, A., Wood, C.M., 2004. Biologically incorporated dietary silver has no ionoregulatory effects in American red crayfish (Procambarus clarkii). Environ. Toxicol. Chem. 23, 388–395. https://doi.org/10.1897/02-572.
Mantel, L.H., Farmer, L.L., 1983. 2 - Osmotic and ionic regulation. In: Mantel, Linda (Ed.), Internal Anatomy and Physiological Regulation. Academic Press, pp. 53–161.
Marigómez, I., Orbea, A., Olabarrieta, I., Etxeberria, M., Cajaraville, M.P., 1996. Structural changes in the digestive lysosomal system of sentinel mussels as biomarkers of environmental stress in mussel-watch programmes. Comp. Biochem. Physiol. C Pharmacol. Toxicol. Endocrinol. 113, 291–297. https://doi.org/10.1016/0742-8413(95)02100-0.
McGillicuddy, E., Murray, I., Kavanagh, S., Morrison, L., Fogarty, A., Cormican, M., Dockery, P., Prendergast, M., Rowan, N., Morris, D., 2017. Silver nanoparticles in the environment: sources, detection and ecotoxicology. Sci. Total Environ. 575, 231–246. https://doi.org/10.1016/j.scitotenv.2016.10.041.
Mehennaoui, K., Cambier, S., Serchi, T., Ziebel, J., Lentzen, E., Valle, N., Guérold, F., Thomann, J.-S., Giamberini, L., Gutleb, A.C., 2018a. Do the pristine physico-chemical properties of silver and gold nanoparticles influence uptake and molecular effects on Gammarus fossarum (Crustacea Amphipoda)? Sci. Total Environ. 643, 1200–1215. https://doi.org/10.1016/j.scitotenv.2018.06.208.
Mehennaoui, K., Georgantzopoulou, A., Felten, V., Andreï, J., Garaud, M., Cambier, S., Serchi, T., Pain-Devin, S., Guérold, F., Audinot, J.-N., Giambérini, L., Gutleb, A.C., 2016. Gammarus fossarum (Crustacea, Amphipoda) as a model organism to study the effects of silver nanoparticles. Sci. Total Environ. 566–567, 1649–1659. https://doi.org/10.1016/j.scitotenv.2016.06.068.
Mehennaoui, K., Legay, S., Serchi, T., Guérold, F., Giamberini, L., Gutleb, A.C., Cambier, S., 2018b. Identification of reference genes for RT-qPCR data normalization in Gammarus fossarum (Crustacea Amphipoda). Sci. Rep. 8, 15225. https://doi.org/10.1038/s41598-018-33561-1.
Minguez, L., Meyer, A., Molloy, D.P., Giambérini, L., 2009. Interactions between parasitism and biological responses in zebra mussels (Dreissena polymorpha): importance in ecotoxicological studies. Environ. Res. 109, 843–850. https://doi.org/10.1016/j.envres.2009.07.012.
Moore, M.N., Halton, D.W., 1973. Histochemical changes in the digestive gland of Lymnaea truncatula infected with Fasciola hepatica. Z. Parasite 43, 1–16. https://doi.org/10.1007/BF00329532.
Nel, A., Xia, T., Mädler, L., Li, N., 2006. Toxic potential of materials at the nanolevel. Science 311, 622–627. https://doi.org/10.1126/science.1114397.
Petersen, E.J., Henry, T.B., Zhao, J., MacCuspie, R.I., Kirschling, T.L., Dobrovolskaia, M. A., Hackley, V., Xing, B., White, J.C., 2014. Identification and avoidance of potential artifacts and misinterpretations in nanomaterial ecotoxicity measurements. Environ. Sci. Technol. 48, 4226–4246. https://doi.org/10.1021/es4052999.
Pipe, R.K., Moore, M.N., 1985. Ultrastructural changes in the lysosomal-vacuolar system in digestive cells of Mytilus edulis as a response to increased salinity. Mar. Biol. 87, 157–163. https://doi.org/10.1007/BF00539423.
Renault, S., Baudrimont, M., Mesmer-Dudons, N., Gonzalez, P., Mornet, S., Brisson, A., 2008. Impacts of gold nanoparticle exposure on two freshwater species: a phytoplanktonic alga (Scenedesmus subspicatus) and a benthic bivalve (Corbicula fluminea). Gold Bull. 41, 116–126. https://doi.org/10.1007/BF03216589.
Rocha, T.L., Gomes, T., Sousa, V.S., Mestre, N.C., Bebianno, M.J., 2015. Ecotoxicological impact of engineered nanomaterials in bivalve molluscs: an overview. Mar. Environ. Res. 111, 74–88. https://doi.org/10.1016/j.marenvres.2015.06.013.
Rosas, C., Sanchez, A., Escobar, E., Soto, L., Bolongaro-Crevenna, A., 1992. Daily variations of oxygen consumption and glucose hemolymph level related to morphophysiological and ecological adaptations of crustacea. Comp. Biochem. Physiol. A Physiol. 101, 323–328. https://doi.org/10.1016/0300-9629(92)90540-7.
Schultz, C., Powell, K., Crossley, A., Jurkschat, K., Kille, P., Morgan, A.J., Read, D., Tyne, W., Lahive, E., Svendsen, C., Spurgeon, D.J., 2015. Analytical approaches to support current understanding of exposure, uptake and distributions of engineered nanoparticles by aquatic and terrestrial organisms. Ecotoxicology 24, 239–261. https://doi.org/10.1007/s10646-014-1387-3.
Scott, G.R., Sloman, K.A., 2004. The effects of environmental pollutants on complex fish behaviour: integrating behavioural and physiological indicators of toxicity. Aquat. Toxicol. 68, 369–392. https://doi.org/10.1016/j.aquatox.2004.03.016.
Smita, S., Gupta, S.K., Bartonova, A., Dusinska, M., Gutleb, A.C., Rahman, Q., 2012. Nanoparticles in the environment: assessment using the causal diagram approach. Environ. Health 11, S13. https://doi.org/10.1186/1476-069X-11-S1-S13.
Sornom, P., Felten, V., Médoc, V., Sroda, S., Rousselle, P., Beisel, J.-N., 2010. Effect of gender on physiological and behavioural responses of Gammarus roeseli (Crustacea Amphipoda) to salinity and temperature. Environ. Pollut. 158, 1288–1295. https://doi.org/10.1016/j.envpol.2010.01.022.
Sørensen, S.N., Holten Lützhøft, H.-C., Rasmussen, R., Baun, A., 2016. Acute and chronic effects from pulse exposure of D. magna to silver and copper oxide nanoparticles. Aquat. Toxicol. 180, 209–217. https://doi.org/10.1016/j.aquatox.2016.10.004.
Tiede, K., Hassellöv, M., Breitbarth, E., Chaudhry, Q., Boxall, A.B.A., 2009. Considerations for environmental fate and ecotoxicity testing to support environmental risk assessments for engineered nanoparticles. J. Chromatogr. A 1216, 503–509. https://doi.org/10.1016/j.chroma.2008.09.008.
Vale, G., Mehennaoui, K., Cambier, S., Libralato, G., Jomini, S., Domingos, R.F., 2016. Manufactured nanoparticles in the aquatic environment-biochemical responses on freshwater organisms: a critical overview. Aquat. Toxicol. 170, 162–174. https://doi.org/10.1016/j.aquatox.2015.11.019.
Vance, M.E., Kuiken, T., Vejerano, E.P., McGinnis, S.P., Hochella, M.F., Rejeski, D., Hull, M.S., 2015. Nanotechnology in the real world: redeveloping the nanomaterial consumer products inventory. Beilstein J. Nanotechnol. 6, 1769–1780. https://doi.org/10.3762/bjnano.6.181.
Vellinger, C., Gismondi, E., Felten, V., Rousselle, P., Mehennaoui, K., Parant, M., Usseglio-Polatera, P., 2013. Single and combined effects of cadmium and arsenate in Gammarus pulex (Crustacea, Amphipoda): understanding the links between physiological and behavioural responses. Aquat. Toxicol. 140–141, 106–116. https://doi.org/10.1016/j.aquatox.2013.05.010.
Volland, M., Hampel, M., Martos-Sitcha, J.A., Trombini, C., Martínez-Rodríguez, G., Blasco, J., 2015. Citrate gold nanoparticle exposure in the marine bivalve Ruditapes philippinarum: uptake, elimination and oxidative stress response. Environ. Sci. Pollut. Res. 22, 17414–17424. https://doi.org/10.1007/s11356-015-4718-x.
Webb, N.A., Wood, C.M., 1998. Physiological analysis of the stress response associated with acute silver nitrate exposure in freshwater rainbow trout (Oncorhynchus mykiss). Environ. Toxicol. Chem. 17, 579–588. https://doi.org/10.1002/etc.5620170408.
Wray, A.T., Klaine, S.J., 2015. Modeling the influence of physicochemical properties on gold nanoparticle uptake and elimination by Daphnia magna. Environ. Toxicol. Chem. 34, 860–872. https://doi.org/10.1002/etc.2881.
Yang, Y., Long, C.-L., Li, H.-P., Wang, Q., Yang, Z.-G., 2016. Analysis of silver and gold nanoparticles in environmental water using single particle-inductively coupled plasma-mass spectrometry. Sci. Total Environ. https://doi.org/10.1016/j.scitotenv.2015.12.150.